

SANDIA REPORT

SAND2004-8184
Unlimited Release
Printed March 2004

Development of Laser Diagnostics for In Situ Measurements of Entrained Particles in Recovery Boilers

Final Project Report

Christopher R. Shaddix and Donald J. Holve

Prepared by
Sandia National Laboratories
Albuquerque, New Mexico 87185 and Livermore, California 94550

Sandia is a multiprogram laboratory operated by Sandia Corporation,
a Lockheed Martin Company, for the United States Department of Energy's
National Nuclear Security Administration under Contract DE-AC04-94AL85000.

Approved for public release; further dissemination unlimited.



Issued by Sandia National Laboratories, operated for the United States
Department of Energy by Sandia Corporation.

NOTICE: This report was prepared as an account of work sponsored by an agency of the United States Government. Neither the United States Government, nor any agency thereof, nor any of their employees, nor any of their contractors, subcontractors, or their employees, make any warranty, express or implied, or assume any legal liability or responsibility for the accuracy, completeness, or usefulness of any information, apparatus, product, or process disclosed, or represent that its use would not infringe privately owned rights. Reference herein to any specific commercial product, process, or service by trade name, trademark, manufacturer, or otherwise, does not necessarily constitute or imply its endorsement, recommendation, or favoring by the United States Government, any agency thereof, or any of their contractors or subcontractors. The views and opinions expressed herein do not necessarily state or reflect those of the United States Government, any agency thereof, or any of their contractors.

Printed in the United States of America. This report has been reproduced directly from the best available copy.

Available to DOE and DOE contractors from
U.S. Department of Energy
Office of Scientific and Technical Information
P.O. Box 62
Oak Ridge, TN 37831

Telephone: (865)576-8401
Facsimile: (865)576-5728
E-Mail: reports@adonis.osti.gov
Online ordering: <http://www.doe.gov/bridge>

Available to the public from
U.S. Department of Commerce
National Technical Information Service
5285 Port Royal Rd
Springfield, VA 22161

Telephone: (800)553-6847
Facsimile: (703)605-6900
E-Mail: orders@ntis.fedworld.gov
Online order: <http://www.ntis.gov/help/ordermethods.asp?loc=7-4-0#online>



SAND2004-8184
Unlimited Release
Printed March 2004

DEVELOPMENT OF LASER DIAGNOSTICS FOR IN SITU MEASUREMENTS OF ENTRAINED PARTICLES IN RECOVERY BOILERS

Final Project Report

Christopher R. Shaddix
Combustion Research Facility
Sandia National Laboratories
Livermore, CA 94550

and

Donald J. Holve
Process Metrix LLC
San Ramon, CA 94583

Abstract

As part of the U.S. Department of Energy (DOE) Office of Industrial Technologies (OIT) Industries of the Future (IOF) Forest Products research program, two different laser diagnostic techniques have been implemented in pulp mill recovery boilers to provide important information on entrained particles. One technique, based on single-particle scattering of a low-power, continuous-wave (cw) laser source, measures the velocity, concentration, and size distribution of particles within the furnace flow, over a predetermined range of particle sizes. For application to recovery boilers, this technique was designed to measure the range of particle sizes known as intermediate size particles (ISPs), roughly from 2–100 μm in diameter. The other diagnostic technique, known as laser-induced breakdown spectroscopy (LIBS), uses a pulsed, high-power laser beam to create a localized plasma spark in the flow, allowing the measurement of the elemental composition of the entrained particles. This technique is most sensitive for particles less than 10 μm in diameter. Implementing these laser diagnostic techniques in recovery boilers proved to be challenging. For the particle scattering measurement, the use of a narrow aperture for measurement of the forward scattered light was postulated and later confirmed to be effective in minimizing background signals associated with the dense sodium fume in the boilers. For the LIBS measurement, a new water-jacketed optics probe was implemented to allow for measurements with an insertion depth of up to two meters in the furnace. Fume particle deposition on the exposed optics at the end of the LIBS probe was problematic but improved with a redesign of the probe geometry and purge flow. Both diagnostic techniques were employed at two representative recovery boilers. The particle scattering diagnostic demonstrated similar trends in mean ISP concentration, ISP size distribution, and temporal variation of ISP concentration at the two boilers. The LIBS measurements showed the presence of a number of major chemical components as well as trace metal elements in the entrained particles.

Table of Contents

Page

Abstract	3
Table of Contents	4
List of Figures	5
List of Tables	9
Acknowledgments.....	10
Executive Summary	11
Background	13
Single Particle Counting	14
Laser-Induced Breakdown Spectroscopy	16
PPC Modifications and Checkout.....	18
LIBS Probe Design and Chemical Characterizations.....	21
Longview Boiler Sampling.....	25
PPC Probe	25
LIBS Probe.....	28
LIBS Probe Head Redesign.....	34
Assessment of PPC Accuracy.....	35
Courtland Boiler Sampling.....	39
PPC Probe	40
LIBS Probe.....	43
Conclusions	45
List of References.....	47

List of Figures

Page

Figure 1.	Schematic diagram of the Process Metrix Process Particle Counter (PPC), with relevant dimensions indicated. The “Test Section” refers to the open slot portion of the probe through which the interrogated flow passes and in which the scattering measurement is performed.....	15
Figure 2.	Photograph of the Process Metrix Process Particle Counter (PPC) optical probe, for particle size and concentration measurements in industrial environments.	16
Figure 3.	Schematic diagram of Sandia’s field-hardened LIBS probe for <i>in situ</i> measurements of entrained particle chemistry in industrial flow systems.....	17
Figure 4.	Photograph of Sandia’s industrial LIBS probe.....	18
Figure 5.	Calculated light scattering response (Lorentz-Mie theory) for the traditional PPC optical geometry, for light-absorbing particles, as a function of particle size and laser illumination wavelength.....	19
Figure 6.	PPC optical configuration, showing the beam block and detection of forward scattered light.	20
Figure 7.	Diagram of the PPC detector light collection geometry, and the relevant angular criteria for determining the particle scattering response function.....	20
Figure 8.	Photographs of the LIBS probe developed for boiler measurements. The photo on the left shows the complete optical probe assembly, alongside the YAG laser and water jacket assembly in which the probe fits. The photo on the right shows a close-up of the probe end, which has local water cooling, a laser focusing lens, and fiber-optic light collection for sparks produced in the center of the slotted flow-through section.	23
Figure 9.	1000-shot average LIBS spectra centered on the primary sodium doublet when sampling sodium particle aerosol streams with different particle loadings.	23
Figure 10.	1000-shot average LIBS spectra when sampling a potassium particle aerosol stream containing 1.9 ppm K and from a solid NaCl sample.	24
Figure 11.	Photograph of the end of the uncooled LIBS probe when interrogating the exhaust of the Multifuel Combustor, when firing black liquor.....	25

Figure 12.	Diagram of the upper furnace and convection pass of the Weyerhaeuser Longview boiler, with sampling locations indicated. All sampling was conducted along the right side of the boiler.....	26
Figure 13.	Photograph of the probe end of the 10-foot long disk impaction probe used to collect particle samples from the boiler flow. The stainless steel sampling disk is 1.85 inches in diameter.	28
Figure 14.	Photographs from an optical microscope of the impaction samples collected at different boiler positions and on different days. Left column shows samples at 7.5x magnification; right column is at 30x magnification. Top row is from the thermoprobe port on Nov. 1, 2000. Middle row is from the same port on Nov. 2, 2000. Bottom row is from the mid-superheater port on Nov. 2, 2000. The thermoprobe port samples were exposed to the flow for 10 s and the mid-superheater samples were exposed for 30 s.....	29
Figure 15.	ISP particle count rate measured by the PPC probe at the thermoprobe port of the Longview boiler, Nov. 1, 2000. Breaks in the count rate plot indicate times between collection of the PPC data.	30
Figure 16.	ISP particle frequency distribution as measured by the PPC probe during sampling in Nov. 2000 at Longview. Squares indicate measurements performed at the thermoprobe port, circles, the port at mid-superheater, triangles, the port at the generator entrance, and diamonds, the port at the economizer entrance.	30
Figure 17.	ISP particle mass distribution as measured by the PPC probe during sampling in Nov. 2000 at Longview. Symbols are as described in Fig. 16.	31
Figure 18.	ISP particle mass distribution as measured at the thermoprobe port by the PPC probe during sampling in Nov. 2000 and May 2001 at Longview. Different symbols denote data collected on different days, with filled symbols indicating sootblowers were activated.....	31
Figure 19.	Logarithmic plot of ISP mass concentration as measured by the PPC probe for different sampling positions in the Longview boiler.....	32
Figure 20.	Photograph of the LIBS furnace sampling probe at the thermoprobe port of the Longview boiler, with the YAG laser and associated umbilicals to the right and the thermoprobe sampling port on the left. A sootblower is housed to the right of the probe.	33
Figure 21.	Example of a one-thousand-shot average (2-minute) LIBS spectra centered at 250 nm in the Longview recovery boiler, with key spectral features labeled.	33

Figure 22.	Simultaneous time traces of quantified LIBS signals for several different chemical elements during sampling at the Longview boiler. The boron, silicon, and manganese signals have been calibrated and are expressed as mg/Nm ³ . The sodium is shown in arbitrary units.	34
Figure 23.	Schematic and photograph of modified LIBS probe end.....	35
Figure 24.	Results of PPC mass balance checks with cement dust. Error bars indicate the variance in mass balance measured for each test.....	37
Figure 25.	Calculated inertial separation number and resultant impaction efficiency as a function of particle size. The efficiency curve with filled circles is for baseline flow and particle conditions, whereas the curve with open squares is for a low impaction condition.....	38
Figure 26.	Comparison of the median ISP mass distribution from the PPC probe to the result from performing automated particle counting and sizing of SEM images of impaction samples. Both PPC and impaction data were collected from the thermoprobe port of the Longview boiler in Nov. 2000. The two curves for inertial correction to the impaction data apply the conditions in Fig. 25 for strong and weak impaction conditions, respectively.....	39
Figure 27.	Photograph of six maintenance beams along the front wall of Courtland recovery boiler #3.	40
Figure 28.	Photograph of Darren Garvis of Process Metrix assisting the insertion of the PPC probe into the Courtland recovery boiler.....	41
Figure 29.	Entrained particle mass size distribution as determined from the PPC probe at the maintenance beam ports of the Courtland boiler. Each line represents the deconvoluted data from a 5-minute sampling period. For comparison, the thicker line shows the median mass PPC dataset from sampling at the thermoprobe port of the Longview boiler.....	41
Figure 30.	Time history of PPC measured particulate mass and superheater tube bank deposit mass at Courtland recovery boiler #3. The PPC mass is given by open squares for 5–100 μm particles and by crosses for 1.2–2.1 μm particles (with mass arbitrarily scaled). The three strain gauge readouts of superheater bank mass are arbitrarily scaled to provide a common starting point.	42
Figure 31.	Photograph of the LIBS probe inserted into a maintenance beam port at Courtland.....	44

Figure 32. Continuous time record of single-shot LIBS peak areas measured in the 250 nm spectral window in the Courtland recovery boiler with a linear spectrometer. The areas have been normalized by local baseline emission strength to correct for variations in the spark strength and detection efficiency. The silicon and manganese peak areas have been offset from boron to clearly display them.....44

Figure 33. One-thousand-shot average LIBS spectrum in the Courtland recovery boiler as recorded on an echelle spectrometer. Identified lines (including LIBS recombination products) are labeled together with the spectral location of the peak line emission in nanometers.....45

List of Tables

Page

Table 1.	Relative Scattering for PPC Geometries and Illumination Wavelengths.....	21
Table 2.	Longview Boiler: Thermocouple and Pitot Tube Measurements of Local Flow Properties, November 2000.....	27
Table 3.	PPC Reticle Measurements	36

Acknowledgments

This project succeeded because of the contributions of a large number of individuals at Sandia and Process Metrix, as well as among our industrial hosts and collaborators at Weyerhaeuser, International Paper, Georgia-Pacific, and McDermott Technology Inc. The assistance of the American Forest and Paper Association (AF&PA) and the Department of Energy was also important. David Ottesen and, later, Shane Sickafoose of Sandia provided expert advice on performing measurements via laser-induced breakdown spectroscopy (LIBS), and Dr. Sickafoose also assisted in analyzing some of the resultant LIBS spectra. Howard Johnsen and Doug Scott, Sandia technologists, performed LIBS tests and calibrations in the laboratory and also performed setup and operation of the LIBS hardware in the field. Sal Birtola, a contract design technician, aided in the original design and subsequent redesign of the long-standoff LIBS probe that was used in the recovery boilers. Sal also designed the water jackets used with the LIBS probe and with the pitot tube/thermocouple probe during the last sampling campaign. Sandia technologist Gian Sclippa assisted with measurements at Weyerhaeuser's Longview boiler, designed and constructed the disk impaction probe, and also operated Sandia's Multifuel Combustor to simulate a recovery boiler flue gas for the LIBS probe and to provide a high-temperature cement dust sampling environment for evaluating the accuracy of the PCSV measurement. Sandia technologist Dennis Morrison assisted with measurements at International Paper's Courtland boiler. Student intern Clay Horiuchi performed optical microscopy on the impaction samples from Courtland. Sandia material scientist Nancy Yang performed SEM on the impaction samples from both boilers. Don Hardesty, Sandia manager, assisted with formulation of the original project proposal.

Michel Bonin of Process Metrix (PM) helped develop the original project proposal and experimental plan. PM's Darren Garvis assisted with calibrations and field operation of the PCSV instrument.

Peter Ariessohn, Bob Roscoe, Bruce Stone, Bill Trout, and Ken Nichols of Weyerhaeuser assisted with various aspects of project planning, mill coordination, boiler testing, and data interpretation.

Jules Dominguez and Karl Morency of Georgia-Pacific assisted with project planning, data interpretation, and evaluation of candidate boilers.

Andy Jones, Sheldon Imrie, and Mike Gregory of International Paper assisted with mill coordination and boiler testing.

Rick Wessel of McDermott Technology Inc. assisted with project planning, data interpretation, and evaluation of boiler operation.

The efforts of all of these individuals, and any we have failed to mention here, are appreciated and were essential to the successful completion of this project.

Executive Summary

This report documents the results of work performed on a project entitled “Laser Sensors for On-Line Monitoring of Carryover in Recovery Boilers,” which was funded by the U.S. Department of Energy (DOE), with industrial cost-share, through the auspices of the Forest Products focus area within the Office of Industrial Technologies (OIT) Industries of the Future (IOF) program. Technical evaluation of the proposed work and of the progress during the course of the project occurred through the American Forest and Paper Association (AF&PA) Agenda2020 Sensors and Control Committee.

The purpose of the project was to adapt two existing industrial laser diagnostic techniques, laser particle counting and laser-induced breakdown spectroscopy (LIBS), to work effectively within the high-temperature, fume-laden environment of a pulp mill recovery boiler. Once operation within recovery boilers had been successively achieved, it was desired to collect data with both instruments in two different recovery boilers, to establish the capabilities of the instruments to yield useful information and hopefully to provide critically needed information on the concentration, size distribution, and chemistry of the small-size portion of entrained particles carried over from the furnace to the convection pass. These particles are intermediate in size between the extensive fume that is generated in recovery boilers and the larger carryover particles, and have come to be known as “intermediate size particles” (ISPs). Sandia National Laboratories and Process Metrix LLC partnered to perform the work in this project. Process Metrix has been developing and applying an industrial laser particle counting technique, now known as the Process Particle Counter (PPC), for over a dozen years. Likewise, Sandia has been developing and applying fieldable LIBS instruments for analysis of entrained aerosols in high temperature flows over the same period of time.

Initial work on the project focused on making modifications to the existing diagnostic techniques and measurement probes to make them operable in the recovery boiler environment, from the upper furnace back through the convection pass. For the laser particle counting technique, the principal barrier to successful implementation in recovery boilers was the large background scattering signature from the high-concentration submicron sodium fume. A computational re-evaluation of the optical design of the probe demonstrated that a substantial reduction in the forward scattering acceptance aperture would provide the requisite discrimination against laser scattering from fume. This modification was implemented and proven in both laboratory and recovery boiler tests to yield the desired performance. For the LIBS technique, spectral detection methodologies for several species needed to be evaluated, a long, water-jacketed probe had to be designed, and the purging of the probe end needed to be improved to implement this technique in recovery boilers. These modifications were performed and the resultant LIBS probe was proven to work in both laboratory and recovery boiler tests, although additional modifications were necessary to improve the effectiveness of purging of the probe end.

Measurements with both the LIBS and particle counting techniques were performed first at a Weyerhaeuser recovery boiler at Longview, Washington, and then at an International Paper recovery boiler at Courtland, Alabama. At Longview, the particle counting probe demonstrated a large variability in the loading of ISP, in part in response to the action of sootblowing. The concentration of ISP was determined to be significant (in comparison to the fume mass concentration) at the entrance to the superheaters and to decline substantially through the convection pass. The mass size distribution of ISP showed a modest growth with size over the

range of 5 to 100 micrometers. LIBS measurements were performed on the elements Na, Mg, C, B, Si, Mn, Ca, Fe, and Cl, with a focus on time traces of the refractory trace metals Si and Mn, together with Na, as an indication of ISP particles in the small spark probe volume.

To gain confidence in the accuracy of the particle counting measurement of ISP concentration, laboratory mass balance checks were performed in both cold and hot laboratory flows with representative mass distribution profiles. The particle counting probe consistently demonstrated a mass balance within 20–30%, consistent with the uncertainty in the reticle calibration for particle sizing. To further evaluate the accuracy of ISP particle size distributions measured with the particle counting probe, impaction plate samples from both Longview and Courtland were evaluated with optical and electron microscopy. After correction for the effect of decreasing impaction efficiency with decreasing particle size, the impaction size distributions showed good agreement with the particle counting measurements.

At the Courtland recovery boiler, measurements were performed just above the nose arch, slightly upstream of the entrance to the superheaters. The ISP concentration and size distribution measured with the particle counting probe were found to be similar to that found upstream of the superheaters at Longview. Strong temporal variations in the ISP concentration were also apparent, consistent with the experience at Longview. A dual-laser particle counting configuration was used at Courtland, allowing the measurement of particles in the size range of 1.2–2.1 μm , in addition to the 5–100 μm range used previously. The smaller particle measurements showed a strong decrease in particle mass loading from 1.2 μm to 2.1 μm , presumably indicative of continued decay of the long-size edge of the fume mass peak. The LIBS measurements at Courtland demonstrated temporal fluctuations in the Si and Mn LIBS signals that were similar to those evidenced at Longview. LIBS measurements with an echelle cross-dispersion spectrometer system demonstrated the ability to detect elemental emission simultaneously over 200–900 nm, but with a reduced sensitivity, particularly at ultraviolet wavelengths, that precluded time-resolved analysis.

In the end, this project resulted in the successful development of a laser particle counting probe and a LIBS probe that worked effectively in pulp mill recovery boilers. These *in situ* measurement techniques were shown to provide rapid information on ISP particle concentrations and size distributions and some portions of particle chemistry. Further work is necessary to enhance the sensitivity of LIBS measurements with broadband spectrometers before a fairly complete, rapid chemical characterization of entrained particles is possible. Weak LIBS signals from chlorine and especially sulfur limit the overall utility of this technique in characterizing important particle chemistry. The ISP concentration and size distribution information from laser particle counting measurements have provided critical data to the recovery boiler research community for assessment of the influence of ISP particle loading on fouling and pluggage of steam tube banks in recovery boilers. In particular, the measured ISP concentrations and size distributions strongly suggest that ISP particles are an important contributor to boiler deposits. Also, the strong variability in ISP particle loading that was revealed by these measurements suggests that improved control of ISP particles is possible, once a better understanding exists of their source(s). Recently, under funding from a different project, the PPC particle counting technique was adapted to provide a measurement of the mass concentration of ultrafine aerosols. Therefore, it should now be possible to construct a PPC probe that simultaneously measures the instantaneous mass of fume and the mass concentration and size distribution of ISP in a recovery boiler.

Background

This report documents the results of work performed on a project entitled “Laser Sensors for On-Line Monitoring of Carryover in Recovery Boilers,” which was funded by the U.S. Department of Energy (DOE), with industrial cost-share, through the auspices of the Forest Products focus area within the Office of Industrial Technology (OIT) Industries of the Future (IOF) program. This project was recommended for funding in 1999 through the Sensors and Control Subcommittee of the American Forest and Paper Association (AF&PA) Agenda2020 program and, subsequent to project funding in late 1999, technical progress was monitored through regular meetings of this same subcommittee.

This project was motivated by the ubiquitous problem of excessive deposit formation in the convection pass of U.S. (and, indeed, all North American) kraft pulp mill recovery boilers. These deposits reduce the energy efficiency of these boilers, limit the pulping capacity of many U.S. kraft pulp mills, and often result in boiler pluggage and lost capacity. The fuel that is burned in the Tomlinson furnace is known as strong black liquor, and typically consists of 20 wt-% sodium (on a dry basis) in a mixture of lignin-derived organics, water, and sulfur compounds [Hupa, 1997]. Combustion of this fuel, both in-flight as a coarse spray and in the upper layers of a char bed on the floor of the furnace, results in the production of a dense cloud of submicron sodium fume particles that are present at very high concentrations (10^7 – 10^9 particles/cm³) in the upper furnace and convection pass portions of recovery boilers. Fume particles have been the focus of a number of detailed particle deposition and physical particle sampling investigations over the years (e.g., see Mikkanen et al., 1998, and Baxter et al., 2001) and their formation mechanisms, chemical evolution, and deposit mechanisms are reasonably well understood. In contrast, available information on the wide range of super-micron particles (from a few microns up to several mm in size) that are present in the flow entering the convection pass is quite limited. These particles are present at a number density (10^2 – 10^4 particles/cm³) far below that of fume particles, but their large size means that they can contribute a significant portion of the entrained particle mass load and they have very high deposition efficiencies. These carryover particles, as they are generally called, are believed to result primarily from upward entrainment of the small-size portion of the black liquor droplets introduced into the furnace. Other potential sources of carryover particles, particularly the smaller size portion of carryover, are droplet fragmentation (ejecta) and particle entrainment from the char bed at the bottom of the furnace. In recent years, particles in the size range between a few micrometers and 100 μ m have become known as intermediate size particles (ISPs). These particles are believed to be too small to have been directly formed from the black liquor spray process. They span the particle size range over which thermophoretic particle deposition, turbulent eddy deposition, and inertial particle impaction have varying degrees of importance through the convection pass.

Deposit growth rates at the superheater and in the first half of the convection pass are thought to be largely controlled by these carryover particles. Laboratory studies have shown that the deposition efficiency of carryover particles is highly sensitive to the size and molten state (i.e., liquid content) of the particles [Shenassa et al., 2001]. The molten state of a particle, in turn, is controlled by the particle temperature and its chemical composition — in particular the chlorine and potassium content [Tran et al., 2002]. Therefore, to accurately assess the importance of ISP on steam tube fouling and tube bank pluggage, measurements are required of ISP concentrations, size distribution, and chemistry in operating recovery boilers. Also, whereas the concentration of fume particles is largely determined by the boiler temperature and the pulping chemistry, ISP particle sizes and concentration are likely controllable by process variables (such as liquor quality, splatter

plate design, and the furnace air distribution) that can be adjusted without strongly affecting overall recovery boiler performance. However, reliable, real-time particle diagnostics that operate effectively in the recovery boiler environment have not been available to ascertain the effect of these process variations on the ISP particle loading. Conventional, extractive sampling of entrained particles in recovery boilers is difficult to perform and interpret, due to the preponderance of submicron sodium fume particles, often in a sticky, semi-molten form in the main flow. The fume coats any exposed, cool probe surface, as well as any larger particles that are sampled into the probe. To-date, the lack of accurate measurements of ISP concentration, size distribution, and composition has limited the understanding of the role of ISP particles in overall deposition rates and superheater corrosion and has limited the reliability of methods used to predict boiler fouling and plugging.

In this project, two laser-based optical diagnostic techniques were adapted for making *in situ* measurements of particles in recovery boilers. These diagnostics promised to provide real-time information on the mass loading and size distribution of ISP particles and the chemical composition of all entrained particles. While robust, both of the techniques employed are relatively expensive, require some training to use effectively, and also require the use of a large, water-jacketed probe (for *in situ* measurements), so it was not anticipated that the end-product of this project would be the development of stand-alone ISP “sensors” that would be readily available for use by boiler operators. Instead, the goals of this project were to develop these diagnostic techniques to collect critical information on entrained particles for the recovery boiler research community and to give pulp mill operators the opportunity to invest in this technology for use at particular mills at particular times. The general operational theory of the two diagnostic techniques is described below.

Single Particle Counting

Process Metrix LLC (formerly, Insitec Measurement Systems) has been at the forefront in the development and application of laser-based particle sizing techniques for *in situ* measurements in industrial environments. For ISP measurements in recovery boilers, the single-particle counting technique is preferred over the measurement of ensemble particle scattering, because of the need to suppress signals from the high fume loading in the flow. In single-particle counting, a laser beam is focused to a small probe volume and individual particle scattering events are measured at a discrete, near-forward scattering angle (see Black et al., 1996, for an overview of laser particle size measurement techniques and Holve and Meyer, 1991, for specifics of the Process Metrix probe design). Lorentz-Mie scattering theory is used to deduce the size of the particle, based on the magnitude of the scattering signal. This approach minimizes sensitivity of the measurement to non-spherical particle shapes. Particle velocities are determined using a time-of-flight calculation of the particle passage through the measurement volume. Variations in the particle trajectories through the laser beam require that the collected intensity signals be analyzed statistically to yield the overall concentration and particle size distribution, through a mathematical deconvolution procedure. The requirement that the preponderance of scattering events involve a single particle limits the number density of particles that can be effectively measured with this technique, depending on the laser focus width (and therefore the maximum particle size to be measured). The strong decrease in particle scattering strength with decreasing particle size also sets a minimum particle size that can be measured (for a given laser beam and detector configuration). To increase the overall size range that can be measured with this technique, a dual laser beam configuration can be used, with one laser’s focus much tighter than the other.

A schematic diagram of the single-particle counter probe developed by Process Metrix is shown as Fig. 1. This probe was known as the Particle Counter, Sizer, Velocimeter (PCSV) at the beginning of this project, but has since been renamed the Process Particle Counter (PPC). A photograph of the optical probe is shown as Fig. 2. Note that the probe geometry is necessarily slotted (with a 4 x 9 cm slot), to allow the process flow to pass through the probe and to allow collection of the forward scattered light from the laser focus, in the middle of the slot. For high-temperature applications, the optical probe is contained within a 10-cm OD water jacket that has a mating slot. This basic probe design has been successfully applied in an 85-MW pulverized-coal-fired boiler [Bonin and Queiroz, 1991, 1996], a commercial chromium plating facility [Bonin and Holve, 1996], and other demanding environments [Black et al., 1996]. Measurements have been performed on particles 0.3 to 300 micrometers in diameter at particle concentrations ranging from sub-part-per-trillion (volume particle/volume gas) to part-per-million levels. For sub-micrometer size classes, the instrument is calibrated with latex spheres. Particles two micrometers and above in diameter are calibrated with a custom optical reticle. This reticle consists of an opaque glass disk with monodispersed discs of known size etched on its surface. The glass disk is rotated through the measurement volume of the PPC, enabling dynamic calibration of the instrument.

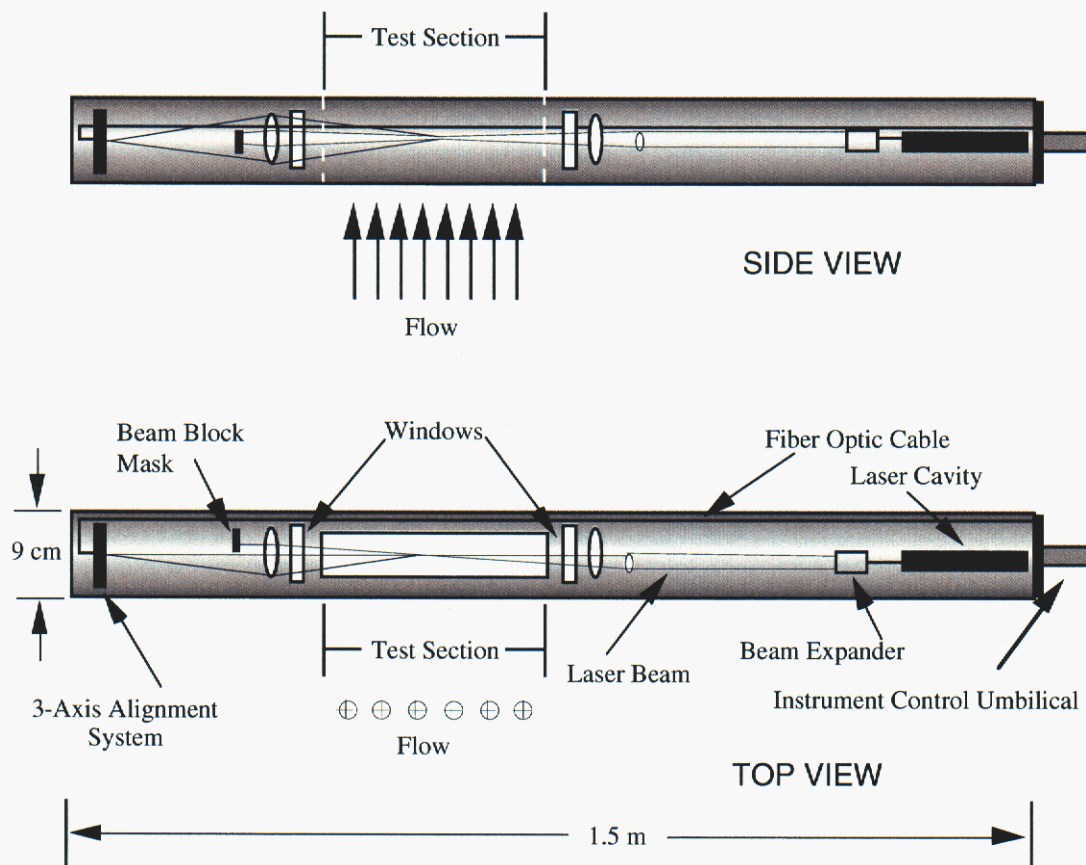


Figure 1. Schematic diagram of the Process Metrix Process Particle Counter (PPC), with relevant dimensions indicated. The “Test Section” refers to the open slot portion of the probe through which the interrogated flow passes and in which the scattering measurement is performed.

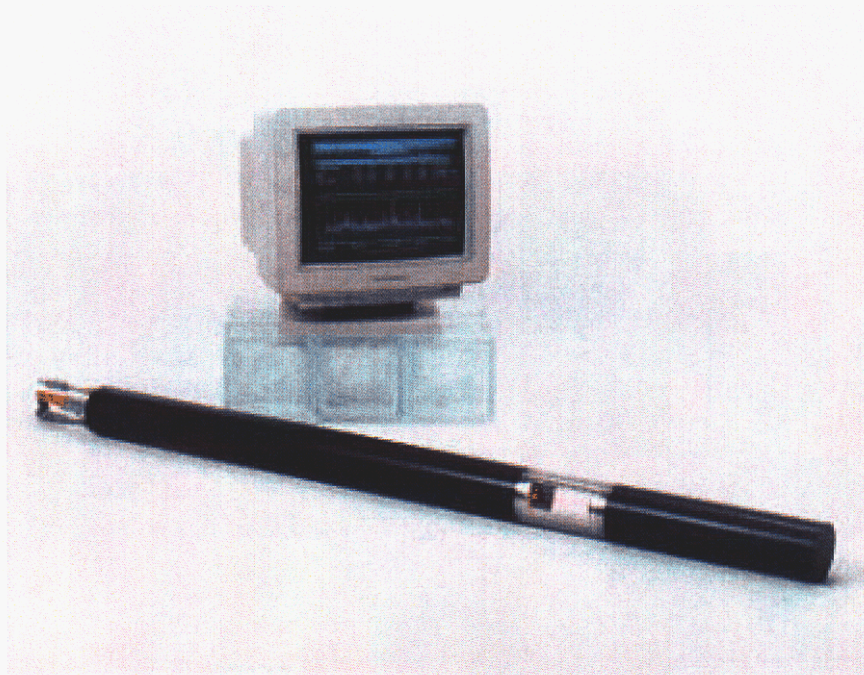


Figure 2. Photograph of the Process Metrix Process Particle Counter (PPC) optical probe, for particle size and concentration measurements in industrial environments.

An existing PPC probe was tested in Weyerhaeuser's Longview, Washington, recovery boiler in 1995, under funding from Weyerhaeuser. This probe demonstrated an ability to survive the harsh chemical and particulate-laden environment of the recovery boiler, but the optical measurements exhibited a strong sensitivity to fume particles relative to larger carryover particles. Consequently, the apparent mass loading of particles in the ISP size range increased through the convection pass (counter to expectations), and the measured particle velocities (~ 1 m/s) were substantially smaller than the local gas flowrates (on the order of 5-10 m/s). In fact, the apparent mass loading of particles in the 20–70 micrometer size range ranged from 20–70 g/Nm³, which is higher than the typical loading of all particulates (including the fume) in recovery boilers. Furthermore, scattering signatures from particles smaller than 20 μm could not be distinguished, because of the large fume scattering background. With this preliminary experience, the first task for the single particle counting diagnostic in this project was to evaluate and implement an improved optical design for discriminating against the high concentration of sodium fume.

Laser-Induced Breakdown Spectroscopy

Laser-induced breakdown spectroscopy (LIBS) is a well-established technique for providing rapid chemical analysis of material samples [Rusak et al., 1997]. LIBS is an atomic emission spectroscopy diagnostic that utilizes a high power, pulsed laser beam as the excitation source. Upon focusing such a laser beam, a spark, or laser-induced plasma, is formed, either at the surface of a large solid object or in a medium containing the sample of interest. Within the laser spark, the molecules and atoms dissociate into electronically excited ions. Ultraviolet, visible, and near-infrared light emission from the excited ions and atoms enables the determination of particle elemental composition from the magnitude and spectral location of light emission from the plasma. Quantitative measurements of overall mass concentrations as well as individual particle

mass and elemental composition have been realized through appropriate analysis and calibration. Quantitative interpretation of LIBS signals from entrained particles is limited to those particles that are completely vaporized and ionized in the laser-induced plasma. The limited studies that have been performed relating to this issue [Cremers and Radziemski, 1985; Carranza and Hahn, 2002a] report upper particle size limits ranging from 2–15 μm for quantitative LIBS signal generation.

Sandia has been using and developing LIBS-based measurement systems since the early 1980's, when laboratory systems were used as research tools for studying gaseous flames and, later, coal combustion [Schmieder, 1982; Ottesen et al., 1989, 1991]. In the early 1990's, Sandia developed a hardened, field-deployable LIBS system, as shown in Figs. 3 and 4, for performing *in situ* LIBS measurements of entrained aerosols under a wide range of industrial operating conditions [Peng et al., 1995]. This laser-optical system was subsequently employed at a number of sites, including the EPA pilot-scale incinerator facility at Research Triangle Park, North Carolina [Hahn et al., 2002], the DOE TSCA Incinerator at Oak Ridge, Tennessee, a chrome-plating facility, several natural gas combustors, and the primary exhaust duct of a production glass melting furnace [Buckley et al., 2000]. The latter test yielded measurements of particulate sodium at concentrations exceeding 15,000 micrograms per cubic meter, together with measurements of calcium, magnesium, silicon, iron, and lithium. This previous field experience of the LIBS probe in industrial environments, particularly at the glass furnace with its substantial sodium fume, gave confidence that the LIBS probe could be used in a recovery boiler.

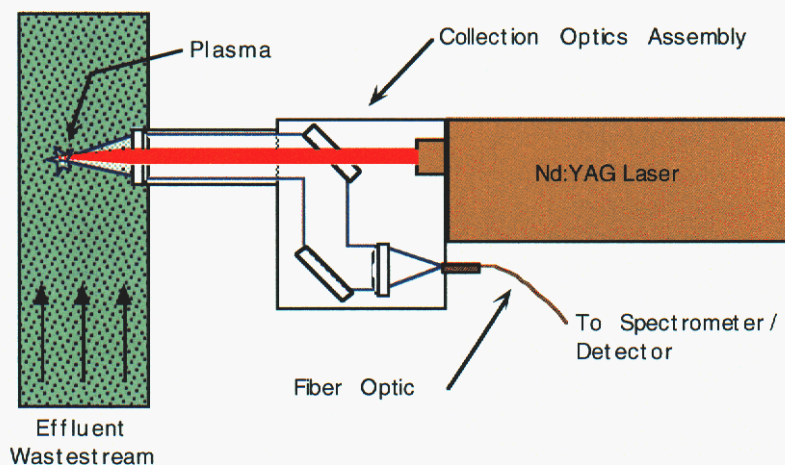


Figure 3. Schematic diagram of Sandia's field-hardened LIBS probe for *in situ* measurements of entrained particle chemistry in industrial flow systems.

Most of the previous LIBS work at Sandia and elsewhere has concentrated on detection and quantification of heavy metal species, especially those whose emissions are regulated under the Resource Conservation and Recovery Act (RCRA) or the Clean Air Act (CAA). These metals also tend to give strong LIBS signals. The important constituents of recovery boiler fume and carryover particles (e.g., Na, K, S, and Cl) involve chemical elements that have not been extensively investigated for detection by LIBS. Consequently, some initial laboratory work on LIBS was necessary in this project to investigate optimum detecting strategies for these elements. Also, the LIBS technique had not previously been applied directly in furnace flows or at large insertion

depths, as desired in recovery boilers, so development work was necessary on these aspects before LIBS could be successfully employed in a recovery boiler.

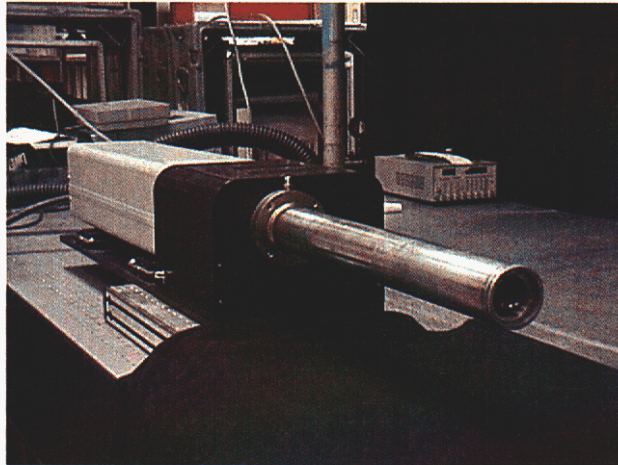


Figure 4. Photograph of Sandia's industrial LIBS probe.

PPC Modifications and Checkout

Based on the unsuccessful particle counting measurements in the mid-1990's at Weyerhaeuser's Longview boiler, it was recognized that a significant modification of the optical system was necessary to minimize contributions from fume scattering in the PPC measurement. At the beginning of this project, it was thought that the most sensible approach would be to change the laser used in the probe to a longer wavelength. As the scattering particle's size falls well below the wavelength of the incident light, the scattered light intensity decreases as D^5 (where D is the particle diameter). Thus, increasing the wavelength of light beyond the visible range, where the wavelength is approximately the same size as the fume particles, will reduce the fume scattering more substantially than that of any larger particles (such as ISP or carryover). In fact, the standard PPC probe design had already increased the laser wavelength from the 633-nm helium-neon laser wavelength that was used in the original Longview measurement campaign to a 670-nm diode laser, but this was not a large enough increase in wavelength to have a substantial effect. Therefore, the original project plan called for the investigation of near-infrared wavelength sources (particularly at 1.55 μm , where there is a large telecommunications laser market) and compatible optics and detectors. If even this wavelength was too short to effectively discriminate against fume, another possibility would be to use mid-infrared lasers, optics, and detectors, but since these lasers and detectors generally require extensive cooling and are not mass-produced, this was seen as a less desirable option. The results of a preliminary analysis of the benefit of using longer wavelength laser sources are shown as Fig. 5. The improvement in the ratio of scattering of a 100 μm particle in comparison to a 1 μm fume particle is equal to 13 in going from a 633 nm laser to 1.55 μm and further improves to 80 for a 3.39 μm laser source. On the other hand, a possible confounding problem for use of infrared wavelengths for detection of scattering is the much higher background thermal radiation (i.e., "blackbody" radiation) that is present at these wavelengths.

Before proceeding to redesign the PPC laser-optical-detector system for infrared operation, however, an evaluation was performed of the choice of forward scattering angle and acceptance

angle for the measurement. This analysis revealed that the traditional PPC optical design could be significantly improved for discrimination against fume scattering by reducing the size of the forward scattering aperture. The PPC optical configuration is shown in Fig. 6 and the scattered light collection geometry is shown in Fig. 7. The standard PPC optical geometry collects scattered light over the entire leftmost portion of the receiver lens shown (in pink) in Fig. 6. This collection geometry balances sensitivity for both large and small particles, allowing measurements (in a dual beam configuration) over 0.3–100 μm , when the total particle concentration is less than 10^6 cm^{-3} . However, for application to measuring ISP particles in the fume-laden environment of the recovery boiler, reducing the acceptance aperture for the scattering measurements and moving it closer to a full-forward position are both beneficial, as they enhance the relative contribution of scattering of large particles relative to fume. Optimizing this new sampling geometry, one finds that the relative improvement in discrimination against fume is actually larger than shifting the laser wavelength from 670 nm out to 1.55 μm , while maintaining the standard detection aperture. This result is shown in Table 1, where it can also be seen that the greatest discrimination against fume scattering occurs for a combination of an optimized detection aperture and a longer laser wavelength.

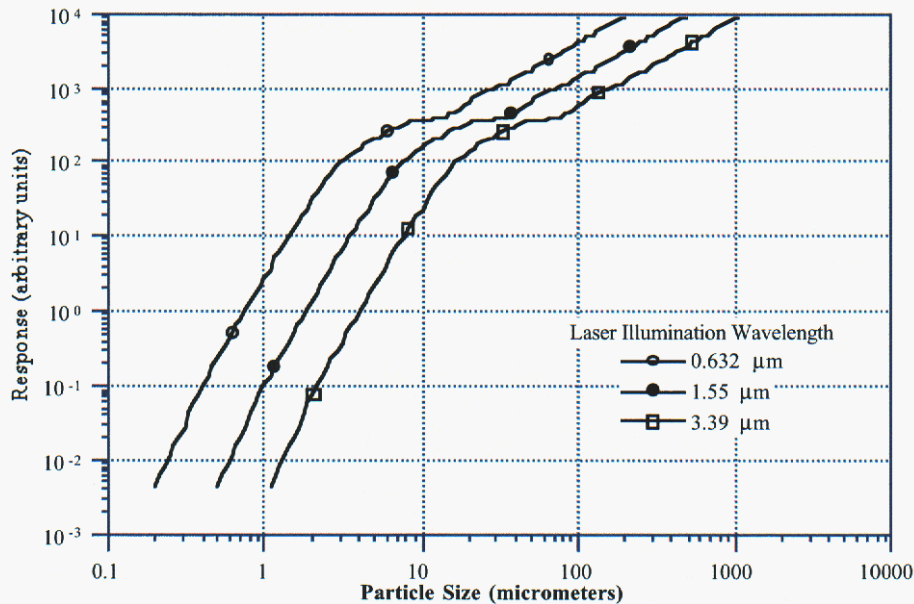


Figure 5. Calculated light scattering response (Lorentz-Mie theory) for the traditional PPC optical geometry, for light-absorbing particles, as a function of particle size and laser illumination wavelength.

Incorporation of a near-infrared laser-optical system into the PPC probe would require significant development time and effort, whereas modifying the detection aperture is inexpensive and easy to implement. Therefore, it was decided that the reduced aperture approach would be seriously explored before making a decision as to the necessity of incorporating the near-IR system. To assess whether the improvement in fume scattering discrimination afforded with the reduced

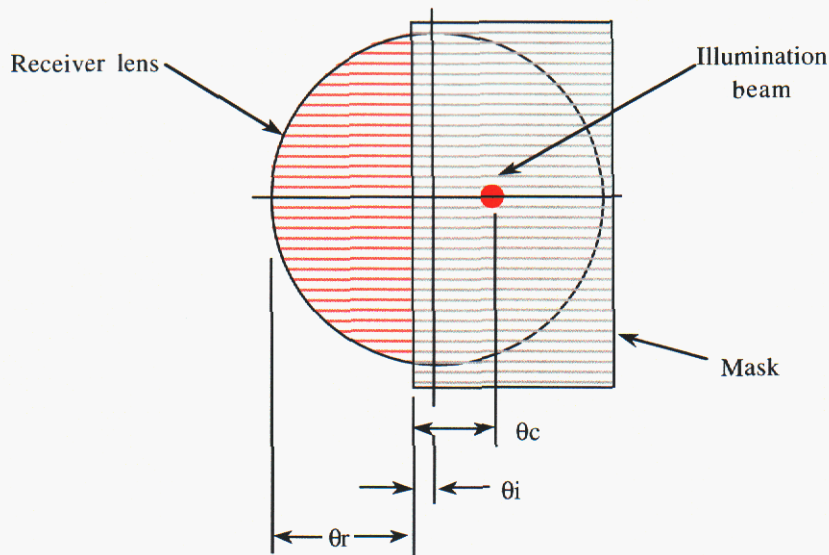


Figure 6. PPC optical configuration, showing the beam block and detection of forward scattered light.

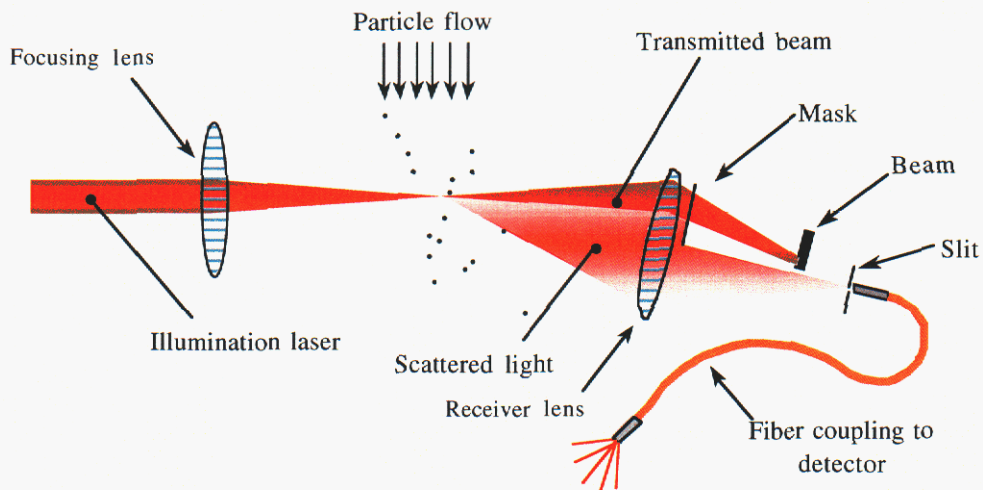


Figure 7. Diagram of the PPC detector light collection geometry, and the relevant angular criteria for determining the particle scattering response function.

aperture approach was likely to be sufficient, mean fume size distribution and concentration data from a recent sampling campaign at the Longview boiler [Baxter et al., 2001] were used to calculate the background scattering signals. With the standard open-aperture PPC detection, the calculated minimum particle size for effective single-particle detection was 26 micrometers, in agreement with the observed lowest measurable particle size of approximately 20–30 μm in the earlier PPC probe test at Longview. In contrast, with the reduced aperture approach, the calculated

minimum detectable particle size was 6 μm . Therefore, it appeared that the reduced aperture modification might be sufficient to allow effective sampling of ISP particles from 5–100 μm .

Once constructed, verification of the operation of the modified PPC instrument was performed using a custom, rotating glass reticle with 2-, 5-, 10-, 20-, 40-, and 80-micrometer particle tracks photo-etched on its surface. These reticle measurements simulate measurements of opaque particles. A plot of measured PPC response versus particle size showed good agreement with Lorentz-Mie theory calculations of the expected instrument response. Further evaluation of the new optical design was performed by re-suspending recovery boiler fume particles (i.e., salt cake) that were collected from the baghouse of Weyerhaeuser’s Longview boiler and entraining them in a 10-cm diameter wind-tunnel with optical access at the Process Metrix research facility. The new PCC instrument demonstrated good discrimination against fume particle scattering and measured an inverse power law size distribution (i.e., rapidly decreasing number density with increasing particle size) between 5 and 55 microns. Five microns is the lower size limit that is measurable with the modified instrument and 55 microns represents the largest size particle measured in this sample. Presumably these larger particles in the salt cake sample represent any carryover that made it to the boiler baghouse, as well as highly agglomerated fume particles.

Table 1. Relative Scattering for PPC Geometries and Illumination Wavelengths

PPC Characteristics	F_{10} (10 μm)	F_1 (1 μm)	Scattering Ratio F_{10}/F_1	Improvement over Std. PPC
Standard PPC: open aperture, 670 nm	375	2.75	136	1
Near-IR PPC: open aperture, 1550 nm	160	0.1	1600	11.8
Reduced Aperture PPC: 670 nm	700	0.275	2545	18.7
Reduced Aperture, Near-IR PPC: 1550 nm	100	0.02	5000	36.8

LIBS Probe Design and Chemical Characterizations

Preliminary discussions with industry representatives and recovery boiler modelers emphasized the need to make boiler measurements with fairly lengthy penetrations into the boiler, to avoid measurement bias from wall effects. A two-meter insertion depth was generally considered to be sufficient to avoid wall effects, while also being practically feasible. Process Metrix has a 4.5 meter long water-jacketed probe that allows PPC measurements to be made at an insertion depth of two meters, with the remainder of the probe functioning as a counterbalance. The industrial LIBS probe that Sandia had developed in the early 1990’s did not incorporate water cooling and was only 0.6 m long. It was designed for accessing exhaust ducts, which are much smaller than boiler spaces

and do not require significant penetration. At the beginning of this project, the optical design of Sandia's existing LIBS probe needed to be assessed for extension to a 3 meter long probe, as was deemed necessary to have a penetration length of two meters. Laboratory experiments were performed that demonstrated that the backprojection technique that Sandia had been using (see Fig. 3) results in significant loss (> 50%) of light collection efficiency for standoff distances greater than 1.5 meters. This is not surprising since the same lens is used for focusing the laser beam (at 1064 nm) that produces the optical breakdown and to collect the emitted light (typ. from 250 to 900 nm for the species in question); as a consequence, the collected light is imperfectly collimated and is not effectively focused onto the spectrometer fiber optic as the standoff distance increases. Two potential solutions to this problem were identified: (a) insertion of a second lens into the existing optical train to partly correct for the imperfect collimation, or (b) use fiber-optic light collection to directly capture the plasma emission near its source. Direct fiber-optic light collection (with a 5-mm diameter, $f/2$ lens) was investigated at angles ranging from forward light collection to backward light collection (somewhat off-axis, because of the laser focusing lens) and in all cases the direct fiber-collected light intensities exceeded those found even with short probe lengths when using the existing backprojection technique.

To apply direct fiber-optic light collection in a single-ended probe, it is desirable to minimize the diameter of the laser-focusing lens. Sandia has traditionally used a laser beam expander to form a YAG beam that is nearly one inch in diameter. This beam is then focused with a two-inch diameter focusing/light collection lens. Laboratory tests demonstrated that the collimation of the expanded YAG laser beam is such that it can be focused with a 25 mm diameter lens, with no noticeable reduction in plasma strength, for probe lengths of 3 meters. Based on these results, a new 3 meter long LIBS probe was designed and constructed for use with a 10 cm OD water jacket. The original intention was to use the same water jacket as had been donated by Weyerhaeuser for use with the PPC probe, but for ease of switching between PPC and LIBS probes when performing boiler sampling, it was determined that it was best to make a duplicate water jacket. Photographs of the long LIBS probe are shown in Fig. 8. Because of the original plan to use the existing water jacket, which is slotted for making the PPC measurements, the LIBS optical probe and water jacket also were initially constructed for the slotted, flow-through geometry. Later, both the optical probe and water jacket were modified to have open-ended sampling.

Preliminary project discussions identified sodium, sulfur, potassium, and chlorine as the primary target species for LIBS measurements of entrained particles in the upper furnace and convection pass regions of recovery boilers. Simultaneous measurements of sodium and sulfur were particularly desired, as such measurements were seen as likely to give useful information on the relative contributions of fume and carryover particles to the detected signals (in the upper furnace and the convection pass the fume is more or less fully sulfated, whereas carryover particles are known to have substantial carbonate content). Previous LIBS measurements by Sandia (e.g., in the exhaust from a glass furnace) showed good sensitivity of the technique to sodium and potassium, but sulfur and chlorine detection had not been extensively investigated by Sandia and had only seen limited investigation by others. LIBS detection of chlorine was evaluated using solid NaCl pellets in air. (LIBS measurements on the surface of macroscopic objects generally provide much higher signals than are possible for entrained particles, because more of the laser pulse energy is coupled into the plasma and into volatilizing and ionizing the elements being interrogated.) Optimal detection wavelength (837.6 nm) and detection gate delay and width parameters (2 μ s and 6 μ s, respectively) were identified. Figs. 9 and 10 show sample spectra from LIBS measurements of

Na, K, and Cl. The sodium measurements are for a range of aerosol concentrations and demonstrate how LIBS calibration curves are constructed for quantifying LIBS signals.

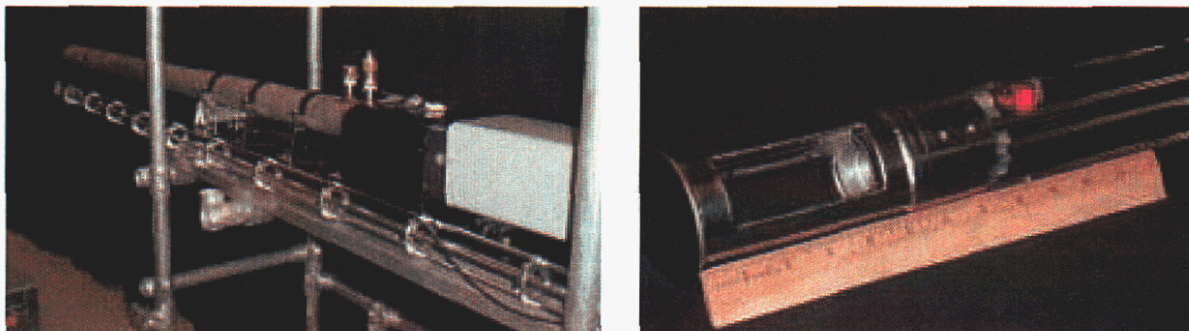


Figure 8. Photographs of the LIBS probe developed for boiler measurements. The photo on the left shows the complete optical probe assembly, alongside the YAG laser and water jacket assembly in which the probe fits. The photo on the right shows a close-up of the probe end, which has local water cooling, a laser focusing lens, and fiber-optic light collection for sparks produced in the center of the slotted flow-through section.

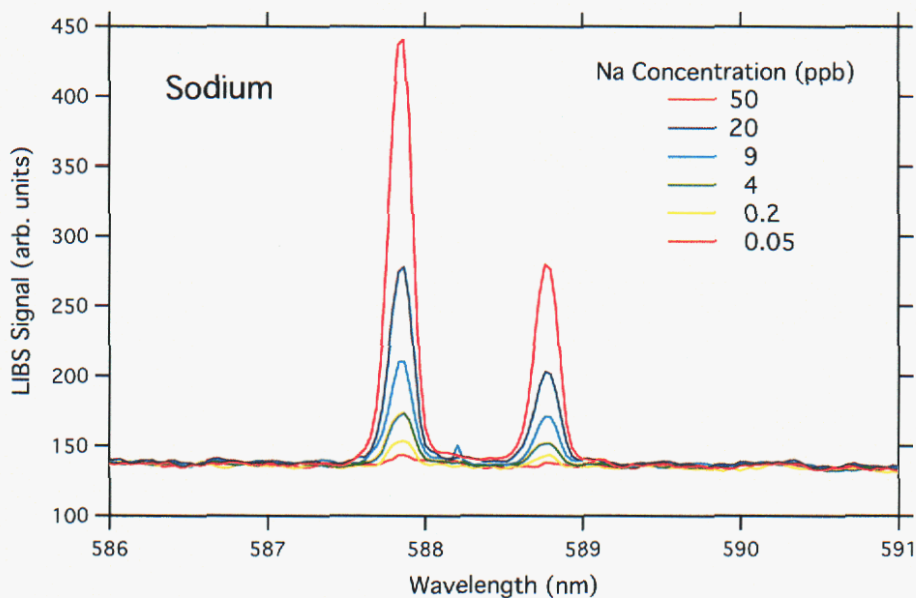


Figure 9. 1000-shot average LIBS spectra centered on the primary sodium doublet when sampling sodium particle aerosol streams with different particle loadings.

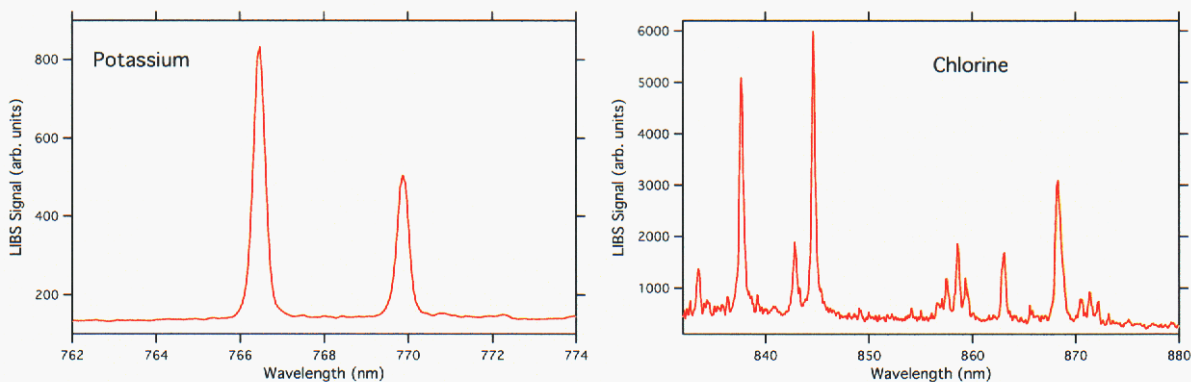


Figure 10. 1000-shot average LIBS spectra when sampling a potassium particle aerosol stream containing 1.9 ppm K and from a solid NaCl sample.

Attempts were made to identify characteristic sulfur emission lines using solid sodium sulfate pellets, entrained sodium sulfate particles ranging in size from 30 to 100 micrometers, and entrained salt cake from the Longview boiler. Unfortunately, no sulfur emission peaks were detected, even when evaluating a wide variety of detection gate delays and sample times. The available literature on LIBS detection of sulfur confirms that the emission lines are very weak and also appear to be sensitive to rapid quenching in air (or presumably any environment with high elemental concentrations of oxygen). Therefore, further testing of sulfur detection was performed, boosting the particle feedrate of Na_2SO_4 until a top sulfur concentration of 12 ppm was developed, and performing the measurements in both an air and a nitrogen carrier gas. The full range of the spectrometer was tested from 190 to 950 nm, but no sulfur signals were detected. Based on measured fume concentrations in the Longview boiler of $\sim 10 \text{ g/Nm}^3$, the expected concentration of sulfur is approximately 2000 ppm, well above what could be produced in the LIBS laboratory tests.

To further explore the detectability of sulfur as well as to simulate the full emission spectrum expected in a recovery boiler, LIBS sampling was performed in the exhaust of Sandia's 35-kW downfired Multifuel Combustor, when firing dilute (20% solids) black liquor. For these measurements, the uncooled, short LIBS probe was used. A photograph of the LIBS probe end and the laser spark in the fume-laden flow is shown in Fig. 11. Spectral surveys revealed the presence of Na, K, and Ca, as expected, as well as Mg, Cl, Fe, B, Si, Mn, Al, and Cu. A subsequent literature search revealed that these latter elements are precisely those non-process elements (NPEs) that are most commonly detectable in black liquors [Grace, 1975]. No sulfur peaks were detectable in the Multifuel Combustor exhaust.

To aid in the discrimination between carryover particle and fume contributions to LIBS signals, a dual spectrometer system was implemented with the use of a bifurcated fiber optic bundle, allowing simultaneous detection of elements with considerably varying detection wavelengths. In this setup, two different 0.275-meter triple-grating monochromators were used. One spectrometer system coupled the grating system to an intensified charge-coupled device (ICCD) with an ultraviolet-extended 1024 x 256 array, whereas the other system coupled the grating system to a 1024-element linear array detector (i.e., an optical multi-channel analyzer, or OMA). Both the fiber-coupled ICCD and OMA systems are sensitive from 200 nm through 900 nm, though the OMA has significantly lower sensitivity than the ICCD. Both systems typically used the 2400 grooves/mm grating, giving a detection window of 35 nm and a spectral resolution greater than 0.1

nm. Further details are provided in Blevins et al., 2003. In the Multifuel Combustor exhaust, the OMA could detect the strong LIBS emitters, Na, K, Ca, and Mg, freeing up the ICCD system for detection of the weaker trace element components.

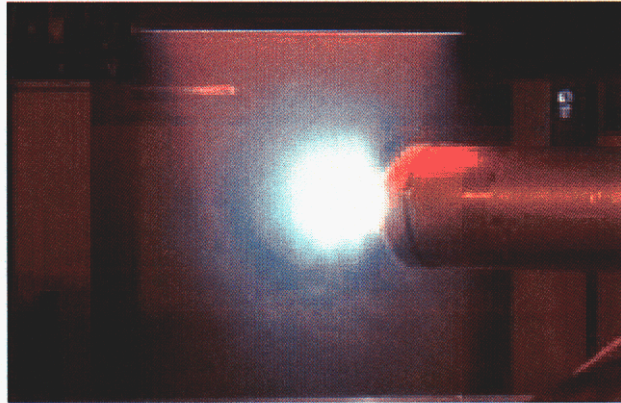


Figure 11. Photograph of the end of the uncooled LIBS probe when interrogating the exhaust of the Multifuel Combustor, when firing black liquor.

Longview Boiler Sampling

PPC Probe

Sampling at Weyerhaeuser's Longview (WA) recovery boiler occurred four different times during the course of this project, between May 2000 and May 2001. The Longview boiler was constructed by B&W in 1975, with an original design capacity of 3.6 MM lbs black liquor dry solids (ds) per day. During the sampling period, the boiler was operating at ~ 4.9 MM lbs ds/day, with a black liquor solids content of ~ 73%. The steaming rate was 755 klbs/hr at 700 psi, and air was delivered to the furnace at 900 klbs/hr via a 3-level air system with a 30-40-30 split. The first two sampling campaigns involved only the PPC single-particle counting diagnostic and largely focused on proving that the reduced aperture PPC probe effectively discriminated against fume scattering and yielded meaningful data on ISP loading. Due to operator concerns over the use of probe cooling water, the first sampling, in May of 2000, was limited to the entrance to the economizer (see boiler diagram in Fig. 12). These measurements confirmed that background fume scattering was low, registering 50–100 mV on the detector output, compared with a 5 μm particle signal of 180 mV. The mean particle velocity measured with the PPC was approximately 4 m/s, which is consistent with expected flow values at this position and therefore gives further credence to the PPC measurements. ISP concentrations determined with the PPC at the economizer entrance were quite low and showed a strong drop in number concentration with increasing particle size. Deduced mass concentrations also decreased with increasing particle size.

After further negotiations between Weyerhaeuser research staff and the mill, a PPC sampling campaign was conducted in Aug. 2000 that included measurements at mid-superheater, the entrance to the generating bank, and the entrance to the economizer. Measurements were planned for a port in front of the superheaters, but that port was found to be welded shut. Measured ISP concentrations and size distributions were similar to those found during the earlier sampling at the economizer, with mid-superheater and generator bank concentrations approximately three times

greater than those at the economizer. The apparent integrated ISP mass concentration at the forward sampling locations was approximately 0.1 g/Nm^3 (grams per cubic meter of volume at 300 K and 101 kPa) in comparison to fume concentrations found during earlier sampling [Baxter et al., 2001] to be roughly 10 g/Nm^3 . The observed laser light extinction in the 3-inch PPC probe slot varied between 20–25%. Calculated fume mass loading corresponding to this extinction is from $5\text{--}10 \text{ g/Nm}^3$, depending on the assumptions one uses for particle extinction efficiency, mean fume particle size, and local gas temperature.

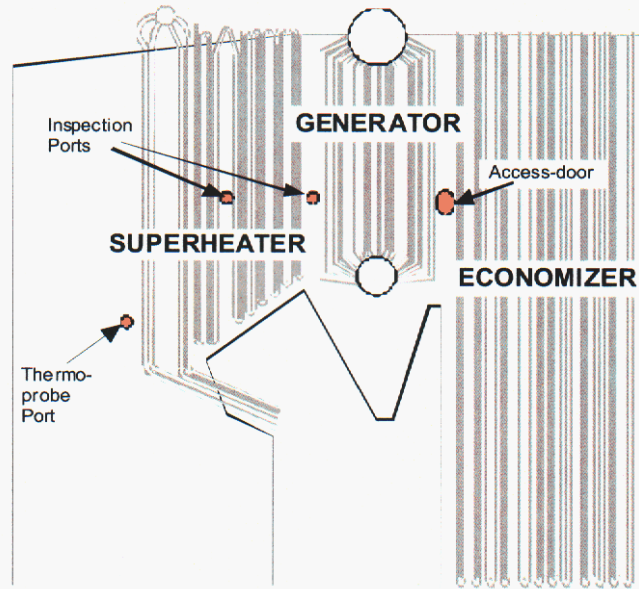


Figure 12. Diagram of the upper furnace and convection pass of the Weyerhaeuser Longview boiler, with sampling locations indicated. All sampling was conducted along the right side of the boiler.

During the August sampling, measurements were taken at both 1-m and 2-m insertion depths and with sootblowers on and off. In general, the ISP particle loading was somewhat higher (by less than a factor of two) when the sootblowers were operating. In addition, the ISP particle count rate in the PPC was observed to increase by up to a factor of ten as a sootblower jet would pass near the PPC probe (count rate increases reflect increases in particle number density, flow velocity, or both of these factors). Subsequent discussions with recovery boiler researchers revealed that sootblower production of ISP within the convection pass had not been previously considered, although with the PPC evidence of this it seems reasonable that the high pressure, high velocity steam sootblower jets would produce a number of fine particles in the process of blowing deposits off of the steam tubes. In this sense it may be appropriate to consider two distinct populations of ISP: (a) “native ISP”, which are formed in the furnace and tend to deposit in the superheater and generator bank, and (b) “sootblower ISP”, which are formed via deposit fragmentation and ablation from sootblowing and which deposit throughout the convection pass.

The third PPC probe sampling campaign at Longview occurred in November of 2000, less than a month after the annual mill shutdown and waterwashing of the boiler. Thus, the steam tube surfaces were expected to be reasonably clean and the penetration of ISP through the convection

pass was likely to be higher than for the previous sampling. By this time, the thermoprobe port just above the nose arch had been opened for use of the 10-cm diameter water-cooled probe. Measurements were taken at 1-m and 2-m insertion depths into the boiler from all four available sampling ports, with duplicate measurements taken on successive days. Because of the limited time allowance for measurements with all of the sootblowers turned off, the majority of the measurements were taken with the sootblower cycle operating normally. Concurrent with the laser measurements of particle concentration, a pitot-tube probe, thermocouple probe, and a particle impaction probe were used to make measurements of gas temperature and velocity and particle properties. As with the previous tests, the new PPC design performed well and showed no significant sensitivity to fume particles, even when sampling the flow in the upper furnace. The mean particle velocities measured by the PPC were found to agree within 10-20% of the velocities measured with the pitot tube. Strong temporal variations in carryover (as diagnosed via the impaction probe) and ISP particle loading (via the PPC probe) were apparent over timescales ranging from a few seconds to days. The local temperature and velocity also showed strong variations over the two-day sampling period, as shown in Table 2. Fig. 13 shows the impaction probe that was used and Fig. 14 shows optical microscopy images of collected impaction samples. The observed strong variations in local flowfield and particle loading were present even though the nominal boiler operating parameters remained constant, suggesting that the primary cause of the variations might be variations in vortical flow through the boiler. Thus, whereas sampling at a given location on one day may happen to occur within the main furnace flow, with higher expected carryover and ISP concentrations, on the next day the sampling ports may be adjacent to a low-flow region.

Table 2. Longview Boiler: Thermocouple and Pitot Tube Measurements of Local Flow Properties, November 2000

Sampling Port	Date	Ave. Temp (°C)	Ave. Velocity (m/s)
thermoprobe port (pre-superheater)	Nov. 1, 2000	920	10.9
	Nov. 2, 2000	820	7.9
mid-superheater	Nov. 1, 2000	620	8.3
	Nov. 2, 2000	710	NA
pre-generator bank	Nov. 1, 2000	520	6.0
	Nov. 2, 2000	490	6.5

As with the previous sampling campaign, the PPC probe showed a strong increase in the ISP particle count rate was evident when a sootblower was operating locally, even when sampling at the thermoprobe port in the upper furnace. This effect is clearly shown in Fig. 15, where the count rate at the thermoprobe port was averaging 170 Hz, with a standard deviation of 40%, when the sootblowers were all turned off, and then averaged 450 Hz, with a standard deviation of 60%, after the sootblowing cycle was resumed. Figs. 16 and 17 present examples of PPC probe measurements of the ISP size distribution, on a number frequency and mass frequency basis. The effects of time variance in ISP loading at a given sampling location and of sootblowing on the concentration of ISPs are suggested in these plots. Once integrated across the full size distribution and corrected for the local gas temperature, the ISP concentration measured in the upper furnace

during this sampling was $\sim 0.5 \text{ g/Nm}^3$ – considerably more than measured further back in the convection pass and an appreciable percentage of the total entrained particulate load (presumably around 10 g/Nm^3).

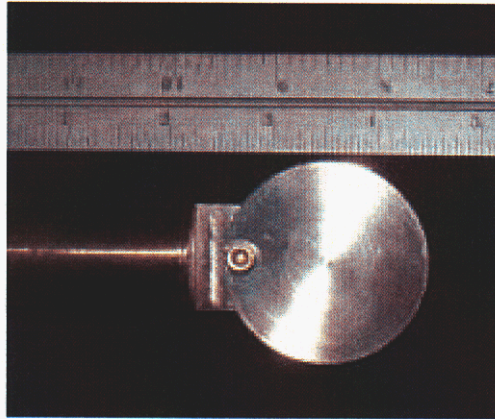


Figure 13. Photograph of the probe end of the 10-foot long disk impaction probe used to collect particle samples from the boiler flow. The stainless steel sampling disk is 1.85 inches in diameter.

To clarify the effects of temporal variance and sootblowing on the ISP load in the upper furnace, a final PPC probe sampling campaign was conducted at Longview in May of 2001, in conjunction with LIBS sampling. This final sampling only utilized the thermoprobe port, to provide as much information as possible about the ISP particles that exit the furnace and enter the convection pass. Fig. 18 shows the results of this final sampling series, together with previously collected mass frequency data from the thermoprobe port. From this data, it is clear that the effects of sootblowing on the ISP population in the upper furnace cannot be distinguished from the inherently large variability of ISP at that location. It is also important to note that there is no evidence of the ISP concentrations varying significantly over the time period of months (in comparison to the level of variability within a given day). The mass size distribution shows a minor peak between 10–20 μm , and then is relatively flat with increasing particle size. Interestingly, the variation in ISP particle loading is particularly pronounced on the large-particle end of the ISP size distribution, where 10-fold variations are apparent, in comparison to 3-fold variations on the small-particle end. Fig. 19 summarizes the total ISP mass concentrations measured with the PPC probe in the Longview boiler. It is apparent that significant loss of ISP occurs through the convection pass (presumably due to deposition on the steam tubes), with most of the mass loss appearing to occur in the superheater bank.

LIBS Probe

LIBS sampling at the Longview boiler occurred during the May 2001 sampling campaign, through the thermoprobe port. A photograph of the LIBS probe and an accompanying support rack is shown in Figure 20. In general, the LIBS diagnostic performed well and data were collected over a number of spectral windows containing emission lines of important major or minor chemical elements expected in the recovery boiler fly ash. Initially, the focusing lens at the end of the LIBS

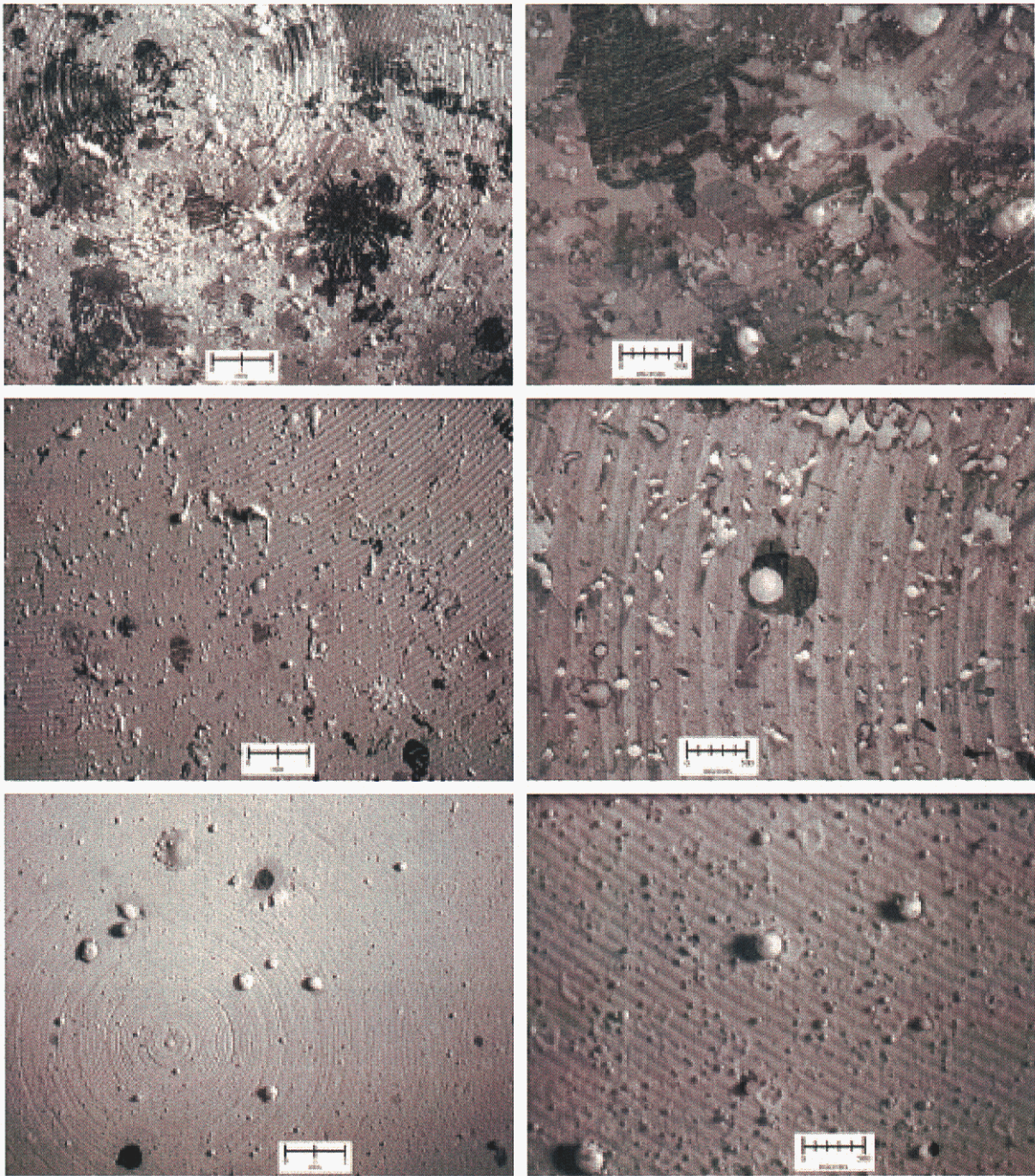


Figure 14. Photographs from an optical microscope of the impactation samples collected at different boiler positions and on different days. Left column shows samples at 7.5x magnification; right column is at 30x magnification. Top row is from the thermoprobe port on Nov. 1, 2000. Middle row is from the same port on Nov. 2, 2000. Bottom row is from the mid-superheater port on Nov. 2, 2000. The thermoprobe port samples were exposed to the flow for 10 s and the mid-superheater samples were exposed for 30 s.

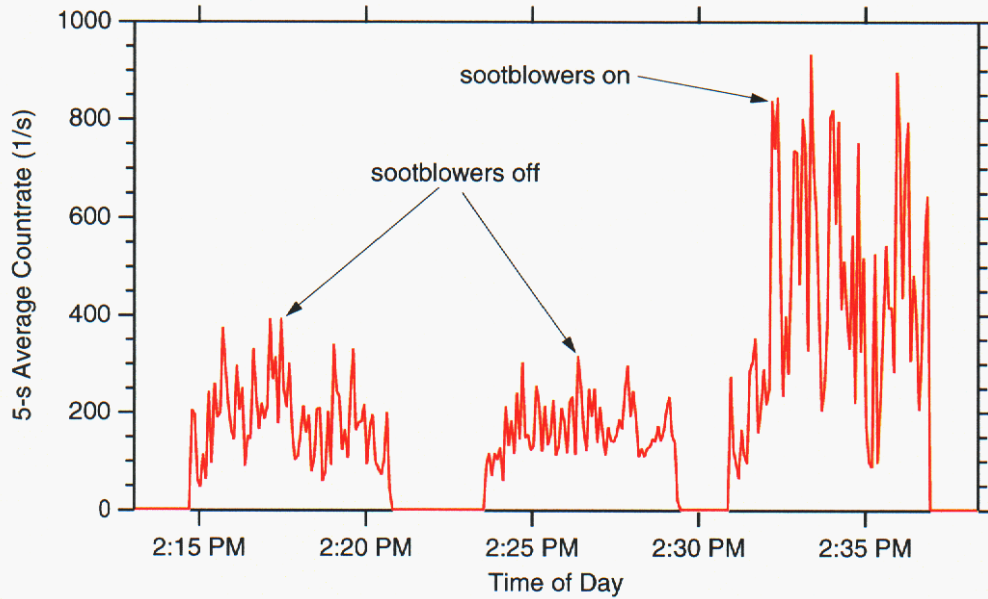


Figure 15. ISP particle count rate measured by the PPC probe at the thermoprobe port of the Longview boiler, Nov. 1, 2000. Breaks in the count rate plot indicate times between collection of the PPC data.

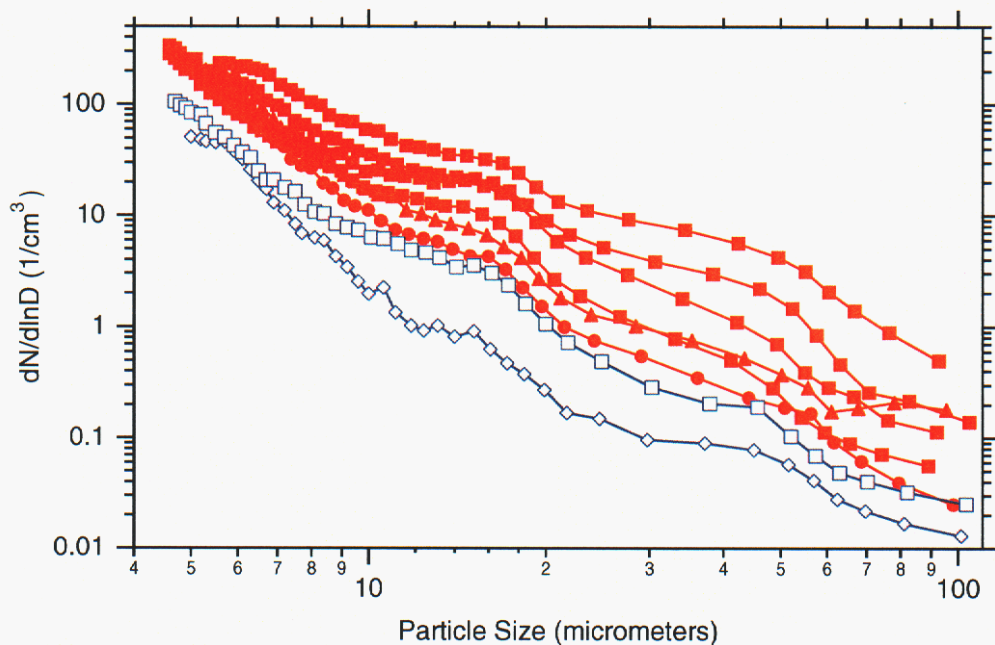


Figure 16. ISP particle frequency distribution as measured by the PPC probe during sampling in Nov. 2000 at Longview. Squares indicate measurements performed at the thermoprobe port, circles, the port at mid-superheater, triangles, the port at the generator entrance, and diamonds, the port at the economizer entrance.

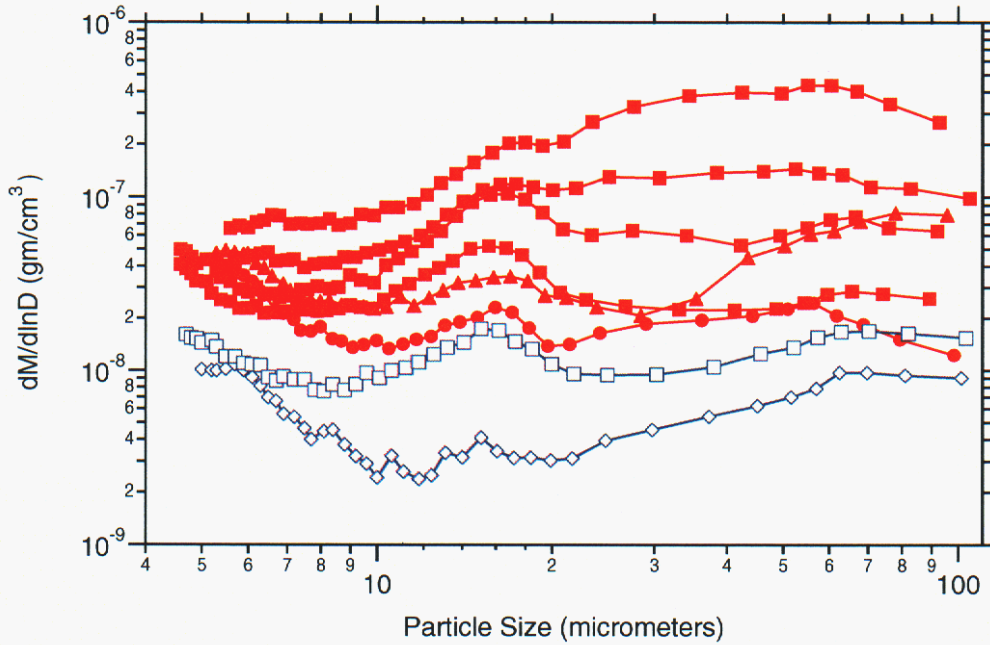


Figure 17. ISP particle mass distribution as measured by the PPC probe during sampling in Nov. 2000 at Longview. Symbols are as described in Fig. 16.

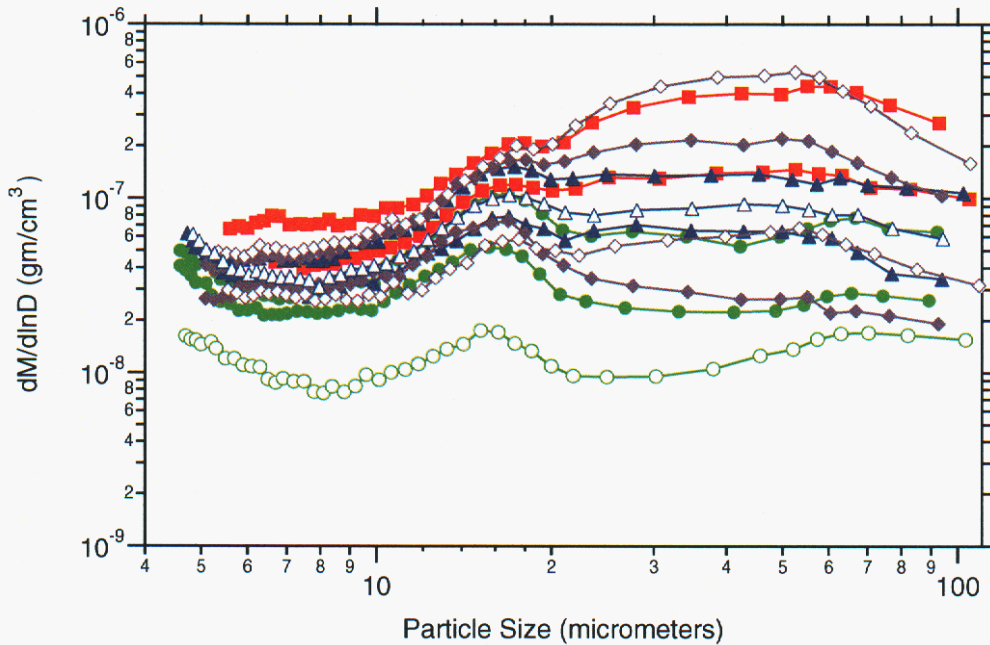


Figure 18. ISP particle mass distribution as measured at the thermoprobe port by the PPC probe during sampling in Nov. 2000 and May 2001 at Longview. Different symbols denote data collected on different days, with filled symbols indicating sootblowers were activated.

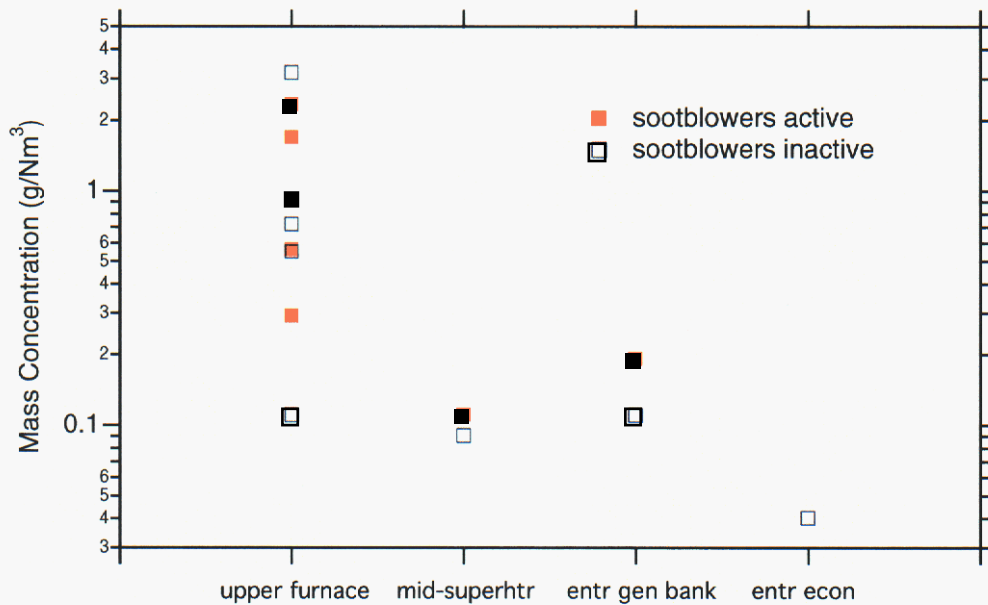


Figure 19. Logarithmic plot of ISP mass concentration as measured by the PPC probe for different sampling positions in the Longview boiler.

probe remained clean and allowed for a 20-minute sampling period, with all of the sootblowers turned off. Later, with shorter periods in which the sootblowers were turned off and with the sootblowers in operation, the focusing lens tended to foul significantly within a few minutes of exposure to the furnace flow, seriously decreasing the LIBS signal strength as the excitation laser strength decreased. Some fouling of the fiber-optic light collector was also found to have occurred. Therefore, the temporal data from Longview tend to have a strong downward drift as a function of sampling time, and limited sampling occurred for different spectral regions during the tests.

Figure 21 shows recovery boiler data from the spectral window centered at 250 nm that was used to simultaneously obtain data on carbon, boron, silicon, and manganese using the spectrometer and ICCD system. Time records of silicon, manganese, and boron, together with sodium, are shown in Fig. 22. The sodium measurement in this case comes from the OMA that was connected in parallel to the ICCD-based spectrometer system. A downward signal trend in the sodium data, due to window fouling, is clearly observed. In addition, the sodium signals show strong shot-to-shot fluctuations in intensity. A recent study of shot-to-shot LIBS signal reproducibility in a homogeneous gas medium showed relative standard deviations of 15% under optimal conditions, increasing to 25% as the limit of optical breakdown is approached [Carranza and Hahn, 2002b]. The even larger shot-to-shot variation observed in the sodium signals from the Longview sampling probably results from a combination of this natural variability in single-shot LIBS signals (particularly with a weakened laser intensity from window fouling and absorption by the fume-laden flow) and variations in the instantaneous fume concentration (and temperature).

The simultaneous data for Si, Mn, and B show some association of strong signals, especially for the refractory elements Si and Mn, but the trends are not definitive. In general, the sodium signals appear to be unrelated to variations in the signals of trace metals such as Si, Mn, and B.

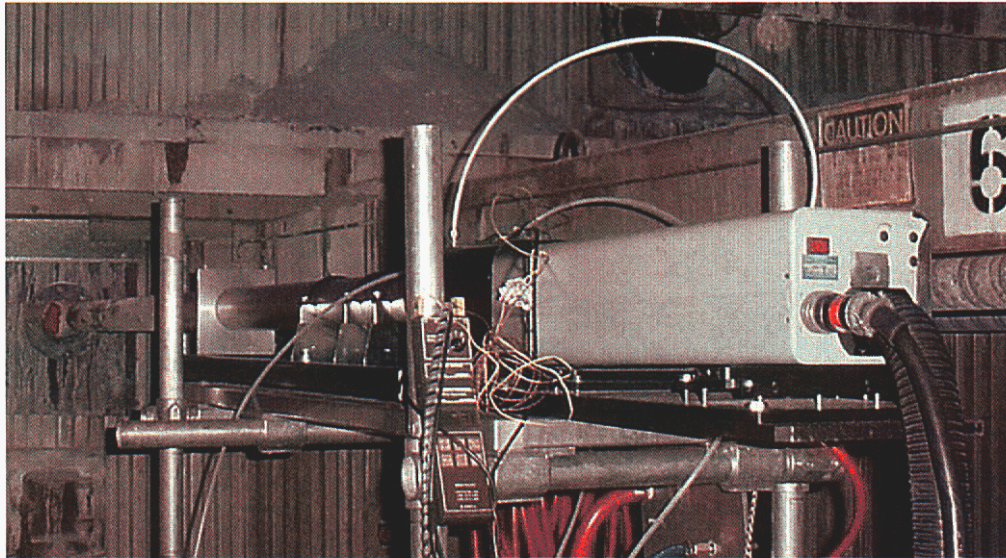


Figure 20. Photograph of the LIBS furnace sampling probe at the thermoprobe port of the Longview boiler, with the YAG laser and associated umbilicals to the right and the thermoprobe sampling port on the left. A sootblower is housed to the right of the probe.

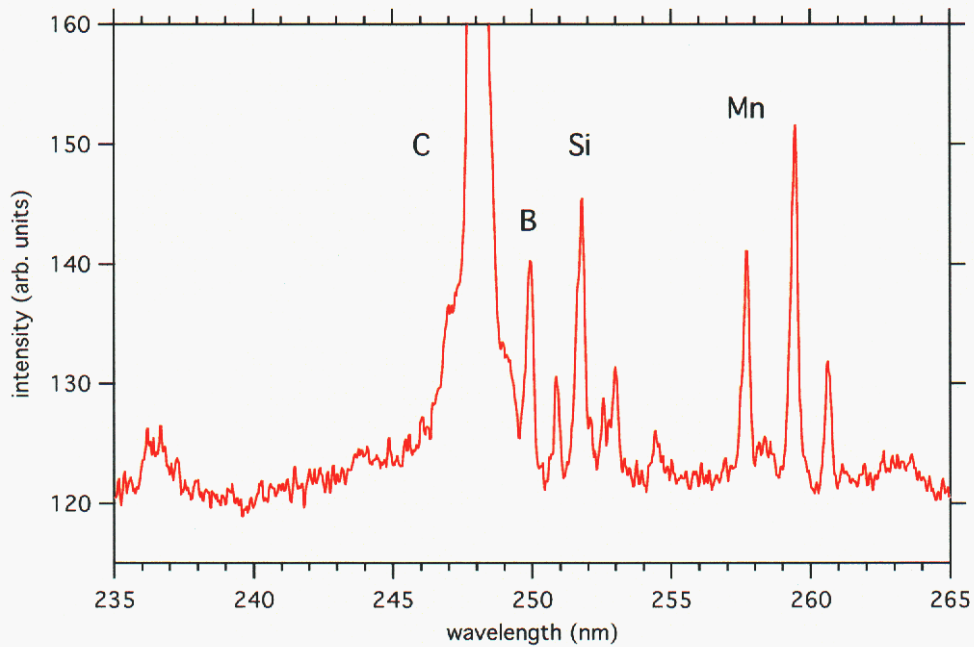


Figure 21. Example of a one-thousand-shot average (2-minute) LIBS spectra centered at 250 nm in the Longview recovery boiler, with key spectral features labeled.

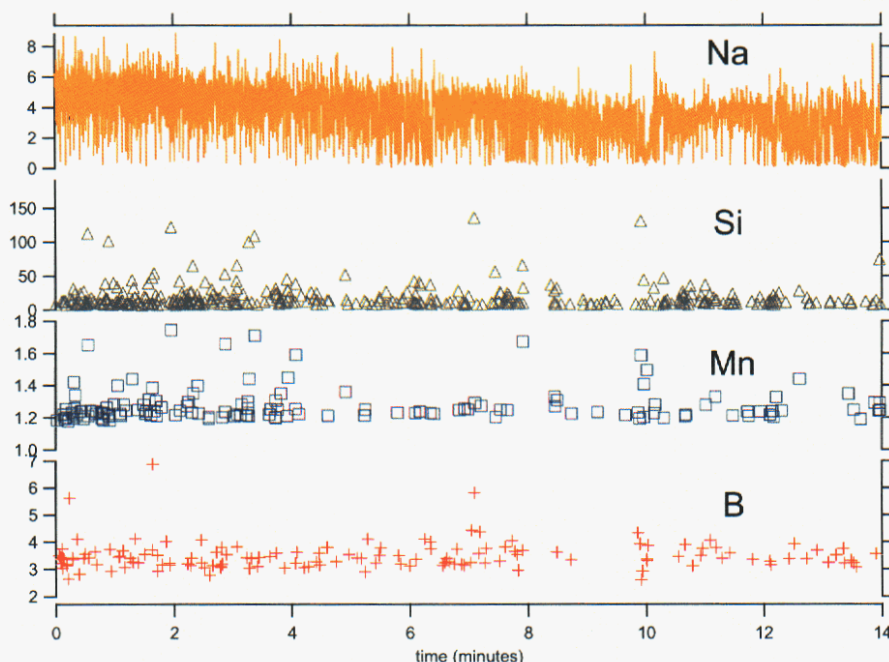


Figure 22. Simultaneous time traces of quantified LIBS signals for several different chemical elements during sampling at the Longview boiler. The boron, silicon, and manganese signals have been calibrated and are expressed as mg/Nm^3 . The sodium is shown in arbitrary units.

In addition to the chemical elements shown in Fig. 21, magnesium gave good signals in the recovery boiler. Calcium, iron, and chlorine signals were all quite weak, and aluminum and sulfur could not be detected. Without sulfur detection, the most promising approach to distinguishing ISP particle contributions from fume particle contributions to the LIBS signal would appear to be monitoring the shot-to-shot concentrations of refractory trace metals, such as silicon and manganese. These constituents are not expected to be significant in fume particles, which are composed solely of compounds that have vaporized and then recondensed. On the other hand, the presumed formation routes for ISP would retain the refractory trace metals that are present in the original black liquor.

LIBS Probe Head Redesign

Based on the difficulty in maintaining the cleanliness of the LIBS laser focusing lens and fiber optic collection lens at Longview, a redesign of the probe end was undertaken. The slotted geometry was removed in favor of an open-ended probe end and the purge flow around the lens was altered to follow a converging conical geometry. The supply line for the purge gas was also enlarged, from 1/8" to 1/4" tubing, to allow a higher flow rate of purge gas for a given purge gas supply pressure available at the boiler. A schematic and photograph of the modified LIBS probe end is shown in Fig. 23.

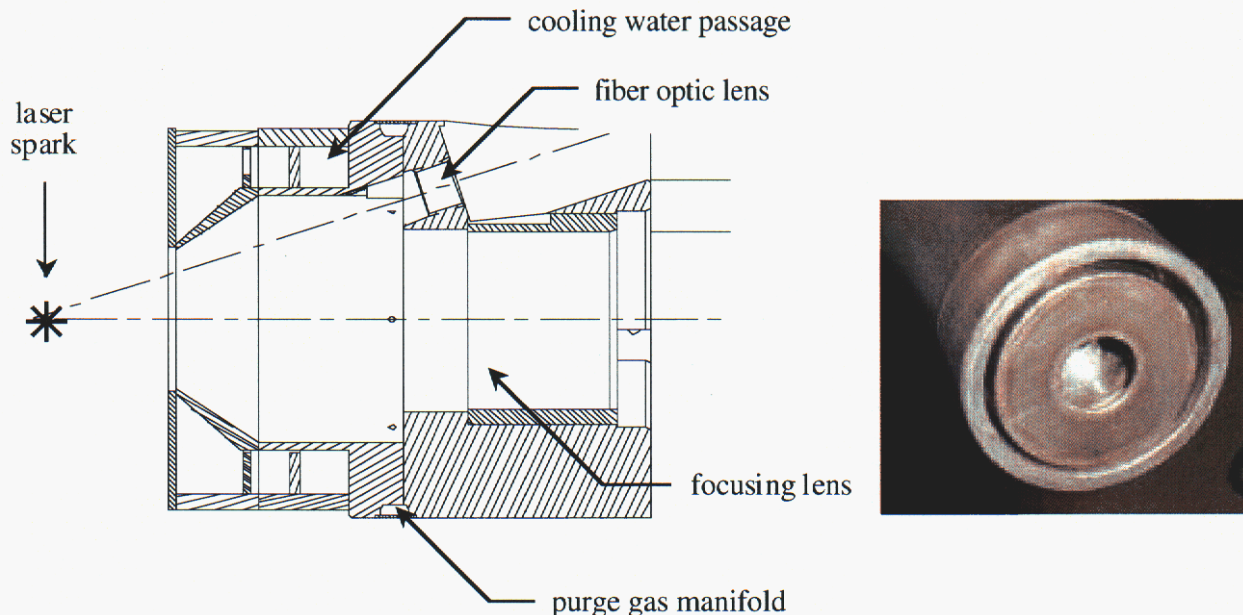


Figure 23. Schematic and photograph of modified LIBS probe end.

Assessment of PPC Accuracy

The ISP particle size distributions and overall mass loading deduced from the PPC probe measurements at the Longview boiler are important for assessments of the importance of the ISP deposition problem and for determining the likely sources of ISP in recovery boilers. However, as with all particle diagnostics, the PPC measurement does have finite uncertainties, associated with factors such as particle shape and density (in translating an effective diameter measurement to mass), flow direction changes, size ambiguity in the flat portion of the response curve, statistical deconvolution of particle trajectory effects, electronic noise, and phantom particles derived from the passage of oversized scatterers. Consequently, during the course of this project a variety of assessments of the PPC measurement accuracy were made, to better quantify uncertainty in its results from recovery boiler sampling.

The standard means of calibrating the scattering signal strength is through the use of optical reticles. Comparing signal strengths before and after a sampling campaign allows one to assess overall optical precision and drift, as it pertains to particle sizing. Table 3 shows the results for 5 different particle artifacts (standard calibration dark field reticles) before and after the May 2001 sampling at the Longview boiler. All but one of the measurements are within 8% of the nominal reticle diameter, and the average deviation is 6% from the nominal diameter.

Achieving a mass balance from known feedrate conditions is arguably the most sensitive check on an optical counter and provides an unambiguous overall validation of the method for the determination of mass loading. For most distributions, a fair portion of the mass is at the top end of the distribution, where the number concentrations are lowest. Thus, number counting errors are primarily statistical sampling errors due to the smaller number of particle counts. These errors can be quantified directly, and are probably less than $\pm 5\%$ for the PPC probe for reasonable sample times. In general, the largest source of error is the size uncertainty due to size calibration errors and uncertainties in the averaged reference beam power. These errors are on the order of $\pm 5\%$, which

translates to a $\pm 15\%$ uncertainty in the mass. These size error estimates are based on spherical particle scattering calculations. In practice, sampled particles may be aspherical, but the large number of particles sampled, coupled with the statistical deconvolution of the data, tends to reduce sizing errors from aspherical particles. This error source is not well quantified, and will depend on the number of particles sampled, the particle size, and the exact shape of the particles. Fortunately, the impact plate samples demonstrate that the ISP particles at the superheater location of the boilers are molten, and therefore are generally spherical. Further back in the convection pass, particle asphericity errors may become significant. The total error in mass, then, is dominated by these sizing errors and is probably in the range of $\pm 20\%$ at the superheater sampling position, and possibly higher further back in the convection pass.

Table 3. PPC Reticle Measurements

Reticle Size (μm , $\pm 3\%$)	PPC Measurement (μm)	
	May 1, 2001	May 8, 2001
5	4.9	5.1
10	10.2	9.3
20	21.5	19.1
40	37	47
80	74	86

Using Portland cement as a surrogate test material, Fig. 24 summarizes total mass measurements of the volume concentration, C_v , obtained in the Process Metrix flow tunnel and the Sandia MFC. Portland cement was chosen as the feed material for these verification tests because its size distribution is similar to the PPC measurements of the ISP size distribution, and 75% of the total mass is within the range of the single-beam PPC used in this project. For the Process Metrix flow tunnel tests, an auger feeder and air eductor was used to mix cement powder at a known feed rate with a primary air flow that was then fed into a 3" diameter pipe, such that all of the flow passed through the flow window of the PPC. The velocity (typically 21 m/s) was measured by the PPC at the centerline of the flow window. The flow velocity at the exit of the 3" wind tunnel was also determined at multiple points in the cross-sectional area by using a water manometer pitot probe. Computing the flow velocity by these two different methods gave results within 10% of each other; the pitot probe measurements were used here because they give the integrated flow velocity across the wind tunnel pipe. For the MFC measurements, the mean velocities measured by the PPC instrument were used to compute the particle mass flux, together with an estimated particle flow diameter in the MFC's open test section. The cement dust apparent density (envelope density of an individual cement particle) was measured by mercury porosimetry ($\pm 10\%$ by Micromeritics analysis laboratory). Using the particle feedrate, the flow data, and the apparent density of the particles, the measured input volume concentration in the flow was computed. The PPC measurements yield results in volume concentration for direct comparison. Fig. 24 shows that the overall mass balance for these various tests was 84%, with a variance of $\pm 17\%$. This level of error and variance in the PPC mass measurements is consistent with the reticle results shown in Table 3 and estimates of particle size calibration and density errors. The PPC variance in these mass balance tests was due primarily to $\pm 5\%$ laser diode power variation and the use of non-spherical cement particles.

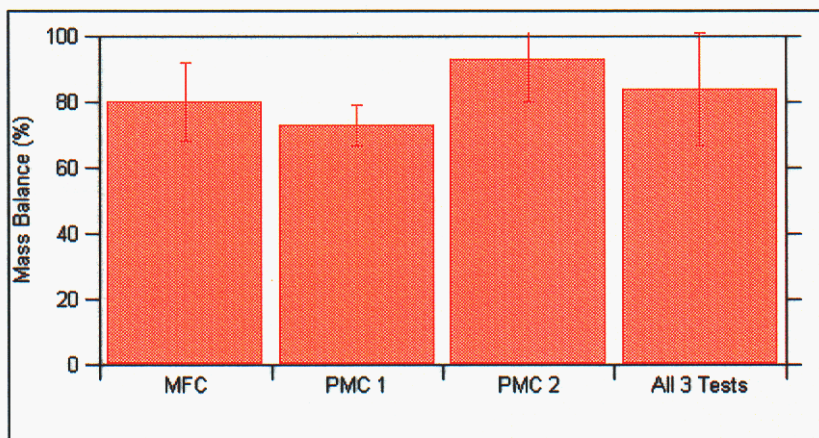


Figure 24. Results of PPC mass balance checks with cement dust. Error bars indicate the variance in mass balance measured for each test.

A more qualitative assessment of the PPC measurement accuracy in recovery boilers (essentially a consistency check) was made by performing a single-particle counting analysis of the impaction plate samples collected at the same sampling ports in the boilers. Analysis of the impaction samples is complicated by impaction efficiencies that vary from zero to nearly one over the size range of ISPs and by uncertainty in the sticking coefficient of the particles onto the plate surface. Interrogation of a number of impaction plates suggests that once a layer of fume has coated the steel plates, the sticking coefficient is nearly one, at least for particles in the ISP size range. This conclusion is based on the observation of relatively few locations where the fume deposit has been diminished or removed completely upon impaction and rebound of a particle. A brief literature review was conducted to assess the state of knowledge of impaction efficiency on round, flat plates, as we have been using to collect impaction samples in the recovery boiler. Surprisingly, no directly applicable analysis was identified. However, a number of studies have been conducted of impaction onto long flat ribbons, as are used in some particulate capture devices. A classic study of this type (Langmuir and Blodgett, 1946, as reprinted in Perry's Handbook of Chemical Engineering) provides the most easily usable information, in the form of curves for impaction efficiency as a function of the inertial separation number. As expected, except for very low values of the inertial separation number, the impaction efficiency on a flat ribbon exceeds that for either a long cylinder or for a sphere, for the same characteristic width. Applying "typical" measured flow conditions at the thermoprobe port during the sampling at Longview ($T = 850\text{ }^{\circ}\text{C}$, $v = 9\text{ m/s}$) and an assumed particle density of 2.6 g/cm^3 (appropriate for nonporous Na_2SO_4), the impaction efficiency drops to zero for particles less than $14\text{ }\mu\text{m}$ in diameter. The complete curve of impaction efficiency versus particle size is shown as Fig. 25. Of course, considerable variability is evident in the flow velocity and temperature in this region of the boiler, and high-resolution SEM images suggest that at least the smaller size portion of ISP particles is composed of fume particle aggregates, with some significant dead space within the aggregates. Hence, at least for some particles and/or size ranges, the impaction curve should be shifted to the right, as indicated in Fig. 25 for the case of an apparent particle density of 1.5 g/cm^3 and a velocity of 6 m/s .

Using low-resolution SEM interrogation of three separate impaction samples, a comparison of the PPC results with the impaction results was made for sampling at the thermoprobe port of the

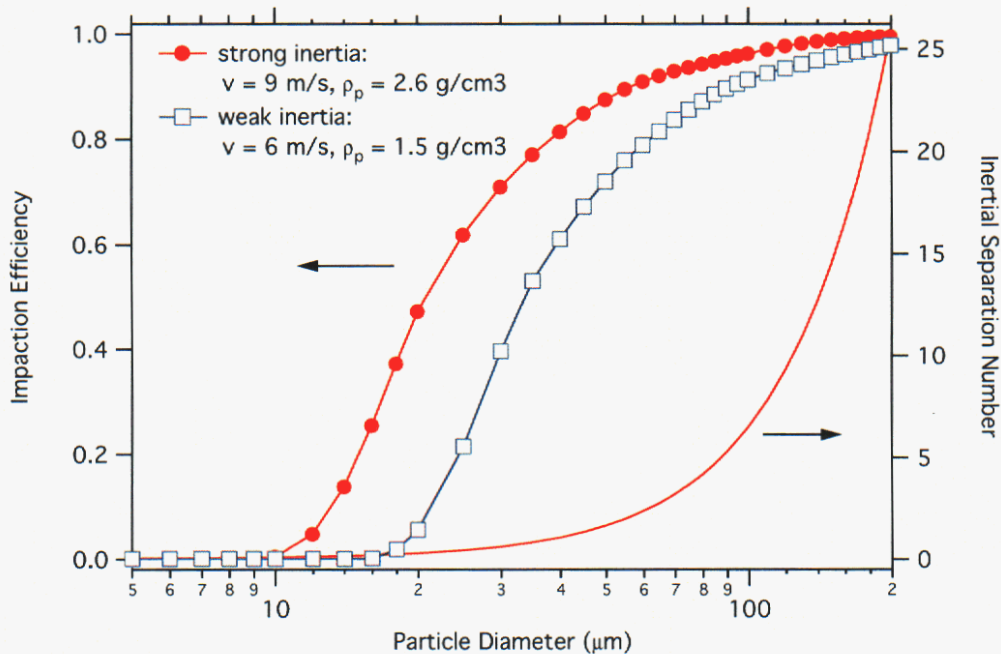


Figure 25. Calculated inertial separation number and resultant impact efficiency as a function of particle size. The efficiency curve with filled circles is for baseline flow and particle conditions, whereas the curve with open squares is for a low impact condition.

Longview boiler, as shown in Fig. 26. The agreement was remarkably good for particle sizes over $40\ \mu\text{m}$, where inertia leads to strong deposition. Accounting for estimates of the inertial deposition efficiency as a function of particle size, the agreement between the PPC measurement and the impaction samples extends somewhat below $40\ \mu\text{m}$, particularly if weak inertia conditions are assumed. A similar comparison between PPC results and impaction sample particle counting was performed for the Courtland boiler, except the impaction plate particle counting was performed manually, using optical micrographs of the impaction plate samples. In this case, the trends in particle size were very similar to those shown in Fig. 26, but the overall particle mass apparent on the impaction samples was about a factor of two lower than the mass measured in a “typical” or mean PPC data sample.

As shown by the impaction mass curve in Fig. 26, a continuum of particles down to the micrometer size range (where fume particles exist) is present on the impaction samples, although the mass contribution of these particles to the deposit mass falls continuously with decreasing particle size. According to the particle impaction calculations shown in Fig. 25, particles below approximately $20\ \mu\text{m}$ at this location in the recovery boiler have insufficient inertia to penetrate through a steady boundary layer and impact the plate. Thus, the small particle deposition on these samples is direct evidence for the unsteady eddy impaction and thermophoretic particle deposition mechanisms that are known to affect particles of this size range. It is also worth noting that the apparent deposition efficiency, as suggested by the ratio of the impaction plate particle mass to the PPC-measured particle mass in the furnace flow, decreases rapidly for particles below $40\ \mu\text{m}$, highlighting the relative deposition efficiency of larger ISP particles in comparison to smaller ISP particles and fume.

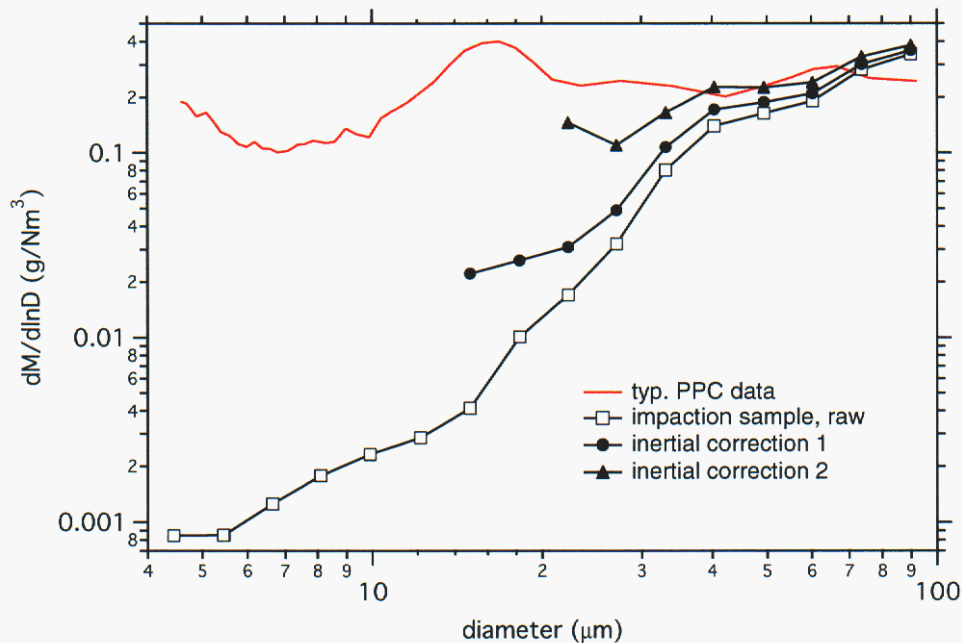


Figure 26. Comparison of the median ISP mass distribution from the PPC probe to the result from performing automated particle counting and sizing of SEM images of impaction samples. Both PPC and impaction data were collected from the thermoprobe port of the Longview boiler in Nov. 2000. The two curves for inertial correction to the impaction data apply the conditions in Fig. 25 for strong and weak impaction conditions, respectively.

Courtland Boiler Sampling

The project plan included particle measurements with the single-particle counting and LIBS techniques at two different recovery boilers, preferably one from the northwest U.S. and one from the southeast U.S. Therefore, even as sampling was first being planned at Weyerhaeuser’s Longview mill, discussions were held with representatives from Georgia-Pacific (GP) on sampling from a boiler at a mill in the southeast U.S. The criteria that were used in identifying appropriate recovery boilers for sampling included (a) mandatory – the availability of one or more large access ports (minimum 4-inch diameter) or manholes in the vicinity of the nose arch, (b) the overall boiler stability and load on the boiler, (c) the modernity of the boiler air handling system, and (d) the ease with which the boiler could be modeled by McDermott Technology Inc. (MTI) personnel. MTI is performing comprehensive boiler modeling to better understand deposit formation from ISP particles as part of a DOE/OIT/FP/Agenda2020 project in the Energy Performance area (“Intermediate-Sized, Entrained Particles in Recovery Boilers: Characterization, Formation, and Control”). Based on these considerations, a GP mill in Ashdown, AR, was considered, which had two different recovery boilers (this mill was subsequently purchased by Domtar Inc.). Meanwhile, discussions with International Paper (IP) revealed a willingness to host a sampling campaign at their recovery boiler #3 at Courtland, AL. This boiler has been performing well, is operated at moderate load, has a modern air handling system and single-drum steam system, and has maintenance beam doors along its front wall for access to the furnace flow just above the nose arch. Furthermore, MTI had recently established a computational grid for modeling

of the Courtland recovery boiler. Based on all of these favorable characteristics, it was ultimately decided to perform the sampling at IP's Courtland mill.

After delays in coordinating plant visits and performing necessary modifications to two of the maintenance beam doors, sampling was performed during the week of August 12, 2002. A photograph of the front wall of the Courtland boiler at the maintenance beam level (just above the nose arch) is shown in Fig. 27. Like the Longview boiler, Courtland recovery boiler #3 was also constructed by B&W. During the sampling campaign, it was operated at a load of 3.9 MM lbs ds/day, which is 93% of the manufacturer's continuous rating (MCR). The black liquor solids content was determined to be 71%. The steaming rate was 530 klbs/hr at 900 psi, and air was delivered to the furnace at 740 klbs/hr via a 3-level air system with a 40-35-25 split. Operation of the furnace was nominally stable throughout the sampling campaign. In contrast to the sampling at Longview, there was no indication (visibly or with any of the measurements) of strong variation in the mean velocity, temperature, or carryover content over time at the sampling ports. Operation of both the LIBS and PPC probes in the Courtland boiler generally went smoothly, despite the significantly higher ambient temperature immediately outside of the boiler, as well as an approximately 100 °C higher temperature inside the boiler, in comparison to the previous sampling at Weyerhaeuser's Longview boiler. All of the LIBS and PPC measurements were made at the maintenance beam level, through one of two available ports, with the boiler sootblowing system operating under its normal schedule.

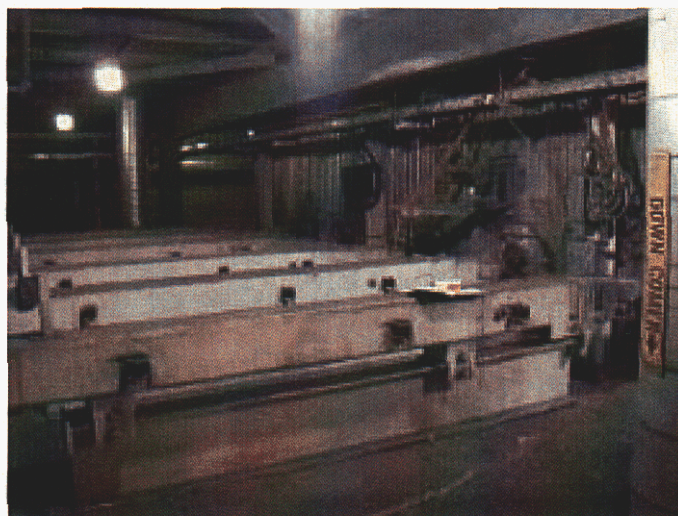


Figure 27. Photograph of six maintenance beams along the front wall of Courtland recovery boiler #3.

PPC Probe

Fig. 28 shows a photograph of the PPC probe entering one of the two available maintenance beam ports at the Courtland boiler. For safety, the maintenance beam doors were retrofitted with a 1-inch thick steel plate in which a 4-inch ID guillotine gate valve was welded. As with PPC sampling at Longview, data were collected over approximately 5-minute long periods. This sampling period was determined to be appropriate for obtaining sufficient particle counts before performing deconvolution of the data. The PPC configuration used at Courtland included two different laser beams, with different focal point waists, which provided a measurement range from 1.2–2.1 μm , in addition to the 5–100 μm range measured with the larger focal waist. As shown in Fig. 29, the

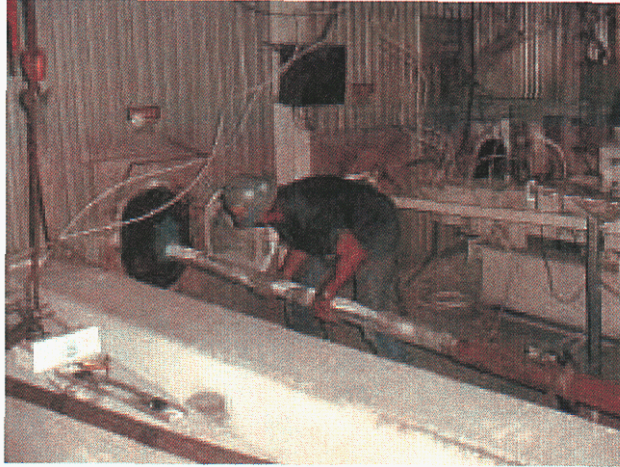


Figure 28. Photograph of Darren Garvis of Process Metrix assisting the insertion of the PPC probe into the Courtland recovery boiler.

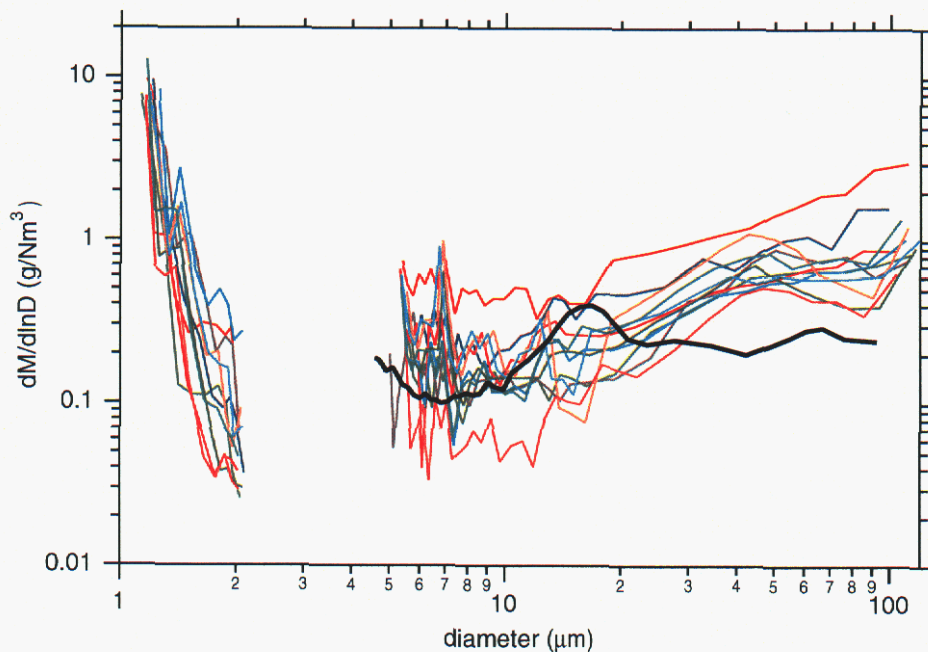


Figure 29. Entrained particle mass size distribution as determined from the PPC probe at the maintenance beam ports of the Courtland boiler. Each line represents the deconvoluted data from a 5-minute sampling period. For comparison, the thicker line shows the median mass PPC dataset from sampling at the thermoprobe port of the Longview boiler.

mass size distribution of the data from 5–100 μm is similar to that from the previous sampling at Longview (where only a single laser beam was used, so the data were limited to this size range). The Courtland data do not tend to show a significant mass peak between 10–20 μm (as the

Longview data showed) and also show somewhat higher mass loading than at Longview for particles greater than 30 μm in size. The Courtland data from the small laser beam show a strong increase in particle mass as the particle size drops below 2 μm . This steeply sloping region presumably is a portion of the large particle end of the fume mass distribution. Both Mikkanen et al. (1998) and Baxter et al. (2001) found recovery boiler fume mass size distributions typically peak at 0.6-0.7 μm in physical size (approximately 1 μm aerodynamic diameter) at a concentration of approximately 25 g/Nm^3 . The fume concentration drops rapidly for larger particle sizes, and is on the order of 0.1-1 g/Nm^3 for Micro-Orifice Uniform Deposit Impactor (MOUDI) stages with size cuts that correspond to 1-2 μm for sodium sulfate particles (Mikkanen, 1998; Baxter et al., 2001). The PPC measured small particle mass distribution in Fig. 29 is consistent with this.

Fig. 30 shows the total mass of particulate measured with the PPC over the size range of 5–100 μm at Courtland, as a function of the time of day in which the data was collected. At the Longview boiler, the total ISP particulate mass over this size range measured with the PPC probe

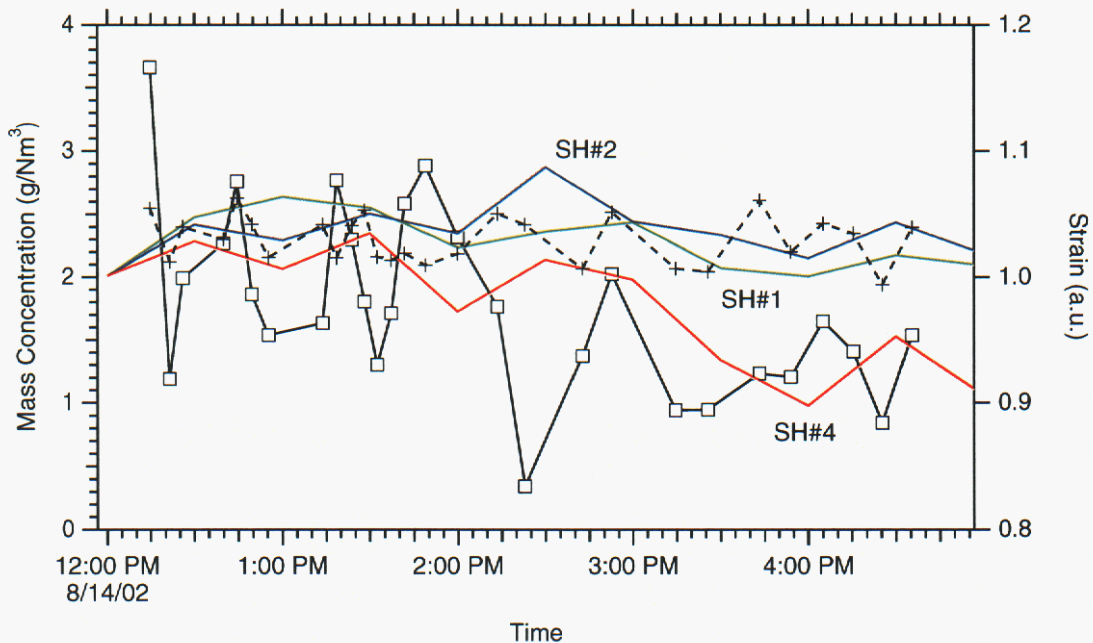


Figure 30. Time history of PPC measured particulate mass and superheater tube bank deposit mass at Courtland recovery boiler #3. The PPC mass is given by open squares for 5–100 μm particles and by crosses for 1.2–2.1 μm particles (with mass arbitrarily scaled). The three strain gauge readouts of superheater tube bank mass are arbitrarily scaled to provide a common starting point.

in the upper furnace (thermoprobe port) varied from 0.1–3.2 g/Nm^3 – so essentially the same range of variability was found in ISP concentrations at the two boilers. Fig. 30 also shows the temporal evolution of the mass concentration of small particles (from 1.2–2.1 μm in size) measured with the PPC and strain gauge measurements from the physical support structures for different tube banks in the superheater. These latter measurements are a new diagnostic that IP has implemented on several of its boilers to give an online indication of the mass loading of deposits

on the steam tubes. It is apparent from Fig. 30 that the small particle concentration (which likely mirrors the total fume concentration) shows a much smaller level of variation in time than the ISP particle concentration. The strain gauge data shows two tube banks whose deposit mass stayed fairly constant in time (like the fume) and another bank that consistently lost deposit mass as the ISP concentration decreased. These trends may be entirely fortuitous, or they may be indicative of relationships between the fume and ISP particle concentrations and deposition patterns in different regions of the superheater. Much longer periods of data collection of this sort would be necessary to accurately identify the relationships between measured particle loading and apparent deposit buildup. The sootblower activation record was examined and compared to the PPC datasets, but no correlation between sootblower location and measured ISP concentration was readily apparent.

LIBS Probe

Some fume deposition on the LIBS probe lens surface did occur at the Courtland boiler, despite the improvements made in the purge flowrate and the probe end design. This deposition limited LIBS sampling periods to approximately ten minutes, but the deposition was significantly reduced relative to what occurred at Longview with the original probe end. A new echelle cross-dispersion spectrometer system was available for use with the LIBS system at Courtland. In contrast to conventional, linear spectrometer systems, with a typical high-resolution spectral window of 35 nm, the echelle spectrometer allows concurrent, high-resolution detection over the entire spectral range from 200-900 nm. Consequently, with an echelle, simultaneous recording of multiple chemical elements should be feasible, including both major components (except sulfur) and trace elements of relevance to recovery boilers. Therefore, it was hoped that with this new detection system the LIBS probe would be able to successfully distinguish chemical signatures from ISP and larger carryover particles from fume. At Courtland, the echelle spectrometer and a conventional linear spectrometer system were simultaneously used to collect data through a bifurcated fiber bundle. The linear spectrometer was maintained at the 250 nm spectral region that had provided interesting information on several trace elements during the sampling in the Longview boiler. A photograph of the LIBS probe when sampling the Courtland boiler flow is shown as Fig. 31.

The temporal variation in the trace metals B, Si, and Mn detected with LIBS was similar to that previously observed at the Longview boiler. Figure 32 shows the trace metal peak area (proportional to concentration) for a typical single-shot LIBS dataset in the Courtland boiler. Some limited correlation is evident in the signals for the refractory metals (Mn and Si). The average cross-correlation coefficients were found to be equal to 0.62 for Mn and Si, 0.34 for Si and B, and 0.58 for Mn and B. With further investigation of LIBS threshold signals for these and other trace metal elements, it may be possible to distinguish ISP particle contributions from fume particle contributions to the LIBS signals. However, incomplete vaporization and ionization of particles greater than 10–20 μm makes quantification of total ISP based on LIBS signals very difficult, if not impossible. Figure 33 shows a sample 1000-shot average spectrum collected with the new echelle cross-dispersion spectrometer system. Strong signals are clearly evident for sodium and potassium. Calcium, titanium, and (surprisingly) rubidium were also identified in the spectrum. Sulfur transitions were not apparent. Trace metal peaks were also generally absent from the echelle spectra, because of this spectrometer's poor sensitivity, particularly in the ultraviolet region. Single-shot echelle spectra could not be effectively captured, because of insufficient sensitivity. Based on this experience, the use of linear spectrometers appears to be preferable over echelle spectrometers for LIBS measurements in recovery boilers, particularly in the UV emission region. If an echelle spectrometer configuration can approach the sensitivity of linear spectrometer systems and allow effective single-shot measurements, then the echelle system would be advantageous.

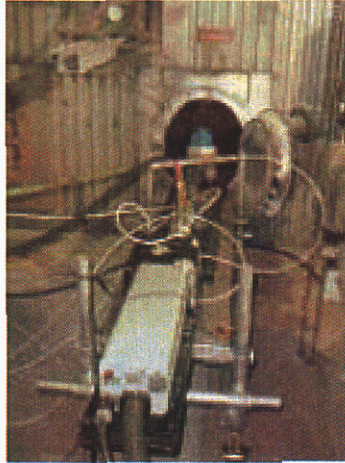


Figure 31. Photograph of the LIBS probe inserted into a maintenance beam port at Courtland.

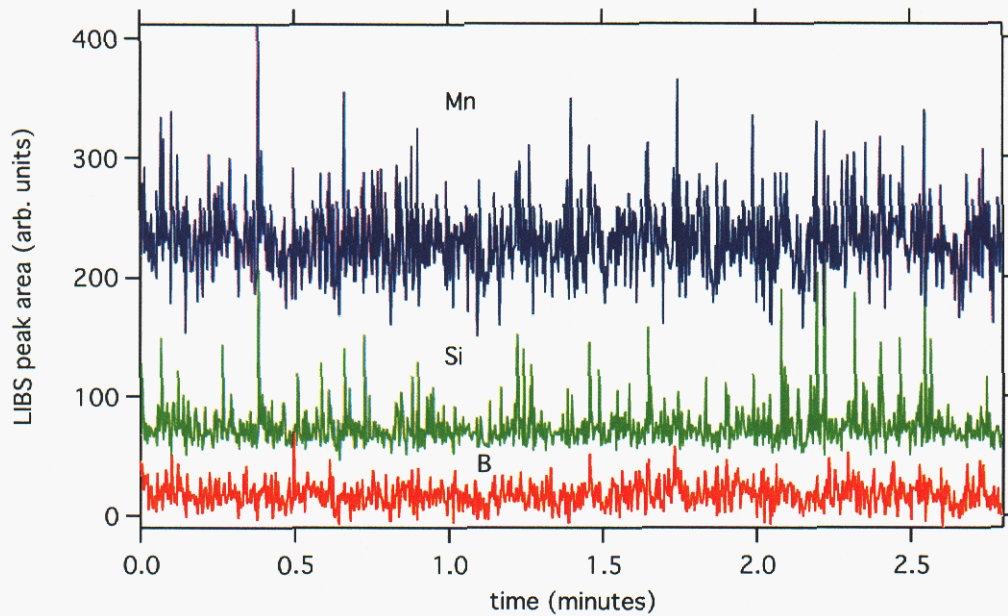


Figure 32. Continuous time record of single-shot LIBS peak areas measured in the 250 nm spectral window in the Courtland recovery boiler with a linear spectrometer. The areas have been normalized by local baseline emission strength to correct for variations in the spark strength and detection efficiency. The silicon and manganese peak areas have been offset from boron to clearly display them.

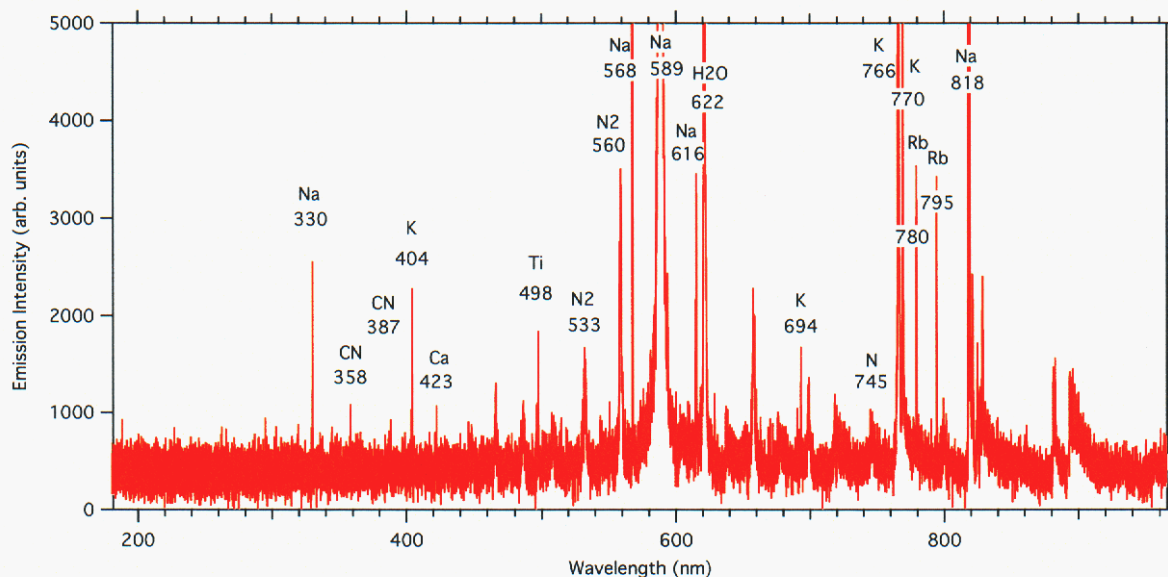


Figure 33. One-thousand-shot average LIBS spectrum in the Courtland recovery boiler as recorded on an echelle spectrometer. Identified lines (including LIBS recombination products) are labeled together with the spectral location of the peak line emission in nanometers.

Conclusions

Two existing industrial laser diagnostic techniques, laser particle counting and laser-induced breakdown spectroscopy (LIBS), were modified during this project to work effectively in the high-temperature, fume-laden environment of a recovery boiler. A modification to the forward scattering aperture in the Process Metrix Process Particle Counter (PPC) probe was found to effectively discriminate against fume scattering and allow quantification of entrained particle distributions from 1.2–100 μm in recovery boilers. With use of this instrument at several sampling ports at the Weyerhaeuser Longview (WA) boiler and at the maintenance beam level of an International Paper Courtland (AL) boiler, critical, previously unavailable information regarding intermediate size particle (ISP) concentrations and size distributions was collected. In particular, ISP concentrations were found to be significant and highly variable at the entrance of the superheater tubes. In traversing the superheater and the generating bank, ISP concentrations drop substantially, presumably because of deposition on the steam tubes. High-pressure steam sootblowing appears to result in the creation of ISP particles as deposits are blown off of the steam tubes. The magnitude of ISP concentrations, their variability, and their mass size distributions were found to be similar at the two boilers sampled.

The LIBS probe required an extensive optical redesign in order to be fitted within a water jacket to collect data with a sufficiently long (3 meter) probe. Laboratory detection optimization was also performed for some elemental constituents of recovery boiler particles. Sulfur detection proved to be impossible with the available detectors and fiber-coupled light collection system. The LIBS probe was used just before the entrance of the superheater tubes at both the Longview and Courtland boilers. Sodium, magnesium, carbon, silicon, manganese, boron, calcium, iron, and chlorine were detected with a linear spectrometer detection system. Temporal variations in the trace

metal components silicon, manganese, and boron were simultaneously recorded and showed some correlation in signals, suggesting a suitable methodology for differentiating between fume and ISP particle contribution to the total signal. An echelle spectrometer system was employed at Courtland and demonstrated simultaneous detection of the LIBS spectra from 200–900 nm, albeit with weak signals in the UV region.

This project has succeeded in developing laser diagnostic techniques that can operate effectively in recovery boilers and give useful information on the size, concentration, and velocity of ISP particles and the elemental chemistry of fume and ISP. A recent extension of the forward scattering technique to measure the concentration of submicron particles should allow the simultaneous measurement of fume particle concentration, together with the properties of ISP. Hence, the diagnostic tools are now available to conduct extensive sampling within recovery boilers to determine the source(s) of ISP and fume and to better control ISP concentrations and resultant steam tube fouling.

List of References

- Baxter, L.L., Lind, T., Rumminger, M., and Kauppinen, E. (2001), "Particle Size Distributions in Recovery Boilers," Proceedings of the 2001 International Chemical Recovery Conference, Whistler BC, Canada, pp. 65–69.
- Black, D.L., McQuay, M.Q., and Bonin, M.P. (1996), "Laser-Based Techniques for Particle-Size Measurement: A Review of Sizing Methods and Their Industrial Applications," *Prog. Energy Combust. Sci.* **22**:267–306.
- Blevins, L.G., Shaddix, C.R., Sickafoose, S.M., and Walsh, P.M. (2003), "Laser-Induced Breakdown Spectroscopy at High Temperatures in Industrial Boilers and Furnaces," *Appl. Optics* **42**(30):6107-6118.
- Bonin, M.P., and Queiroz, M. (1991), "Local particle velocity, size, and concentration measurements in an industrial-scale pulverized coal-fired boiler," *Comb. Flame* **85**:121–133.
- Bonin, M.P., and Queiroz, M. (1996), "A parametric evaluation of particle-phase dynamics in an industrial pulverized-coal-fired boiler," *Fuel* **75**(2):195–206.
- Bonin, M.P., and Holve, D.J. (1996), "Measuring particle size and concentration emissions from electroplating processes," *Metal Finishing*, Oct., pp. 37–41.
- Buckley, S.G., Walsh, P.M., Hahn, D.W., Gallagher, R.J., Misra, M.K., Brown, J.T., Tong, S.S.C., Quan, F., Bhatia, K., Koram, K.K., Hinery, V.I., and Moore, R.D. (2000), "Measurements of Sodium in an Oxygen-Natural Gas Fired Soda-Lime-Silica Glass Melting Furnace," *Ceramic Engineering and Science Proceedings* **21**:183-205.
- Carranza, J.E., and Hahn, D.W. (2002a), "Assessment of the Upper Particle Size Limit for Quantitative Analysis of Aerosols using Laser-Induced Breakdown Spectroscopy," *Anal. Chem.* **74**:5450-5454.
- Carranza, J.E., and Hahn, D.W. (2002b), "Sampling Statistics and Considerations for Single-Shot Analysis using Laser-Induced Breakdown Spectroscopy," *Spectrochim. Acta Part B* **57**:779-790.
- Cremers, D.A., and Radziemski, L.J. (1985), "Direct Detection of Beryllium on Filters using the Laser Spark," *J. Appl. Spectrosc.* **39**(1):57-63.
- Grace, T.M., IPC Project 3234, Report 1 (1975).
- Hahn, D.H., Buckley, S.G., and Johnsen, H., "Laser-Induced Breakdown Spectroscopy Continuous Emissions Monitor for Metals," DOE Office of Science and Technology Innovative Technology Summary Report DOE/EM-0645, Tech ID 18, September 2002.
- Holve, D.J., and Meyer, P.L., "In Situ Particle Measurements in Combustion Environments," in Combustion Measurements (N. Chigier, Ed.), Hemisphere Publishing, New York, c. 1991.

- Hupa, M., "Recovery Boiler Chemistry," in Kraft Recovery Boilers (T.N. Adams, Ed.), TAPPI Press, Atlanta GA, c. 1997.
- Langmuir and Blodgett, U.S. Army Air Forces Tech. Rep. 5418, Feb. 19, 1946 (U.S. Dept. of Commerce, Office of Tech. Services PB 27565).
- Mikkanen, P., Kauppinen, E. I., Pyykönen, J., Jokiniemi, J. K., Aurela, M., Vakkilainen, E. K., and Janka, K. (1998), "Alkali Salt Ash Formation in Four Finnish Industrial Recovery Boilers," *Energy & Fuels* **13**:778–795.
- Ottesen, D.K., Wang, J.C.F, and Radziemski, L.J., (1989), "Real-Time Laser Spark Spectroscopy of Particulates in Combustion Environments," *Appl. Spectros.* **43**(6):967–976.
- Ottesen, D.K., Baxter, L.L., Radziemski, L.J., and Burrows, J.F. (1991), "Laser Spark Emission Spectroscopy for In Situ, Real-Time Monitoring of Pulverized Coal Particle Composition," *Energy & Fuels* **5**(2):304–312.
- Peng, L.W., Flower, W.L., Hencken, K.R., Johnsen, H.A., Renzi, R.F., and French, N.B. (1995), "A Laser-Based Technique for Continuously Monitoring Metal Emissions from Thermal Waste Treatment Units," *Process Control and Quality* **7**:39–49.
- Rusak, D.A., Castle, B.C., Smith, B.W., and Winefordner, J.D. (1997), "Fundamentals and Applications of Laser-Induced Breakdown Spectroscopy," *Crit. Rev. Anal. Chem.* **27**:257–290.
- Schmieder, R.W., "Combustion Applications of Laser-Induced Breakdown Spectroscopy," Sandia Report, SAND81-8886, March 1982.
- Shenassa, R., Kuhn, D.C.S., and Tran, H. (2001), "The Role of Liquid Content in Carryover Deposition in Kraft Recovery Boilers – a Fundamental Study," Proceedings of the 2001 International Chemical Recovery Conference, Whistler BC, Canada, pp. 301–305.
- Tran, H.N., Mao, X., Kuhn, D.C.S., Backman, R., and Hupa, M. (2002), "The Sticky Temperature of Recovery Boiler Fireside Deposits," *Pulp & Paper Canada* **103**(9):29–33.

Distribution

- 5 Dr. Donald Holve
Process Metrix LLC
2110 Omega Rd., Suite D
San Ramon, CA 94583
- 1 Dr. Peter Ariessohn
Enertechnix, Inc.
5412 180th Avenue East
Sumner, WA 98390
- 1 Elmer Fleischman
Idaho National Energy & Engineering Lab
MS 3815
P.O. Box 1625
Idaho Falls, ID 83415
- 1 Dr. Richard Wessel
Babcock & Wilcox Co.
20 S. Van Buren Ave.
P.O. Box 351
Barberton, OH 44203-0351
- 1 Dr. Chris Verrill
Institute of Paper Sci. & Tech.
500 10th Street NW
Atlanta, GA 30318-5794
- 1 Professor Honghi Tran
Dept. of Chemical Engring & Appl. Chem.
University of Toronto
200 College Street
Toronto, Ontario M5S 3E5
CANADA
- 1 Professor Larry Baxter
Dept. of Chemical Engineering
Brigham Young University
350 Clyde Building
Provo, UT 84602

Sandia Distribution

- 1 MS 9054 W.J. McLean, 8300
1 MS 9054 D.R. Hardesty, 8360
1 MS 9052 J.O. Keller, 8367
5 MS 9052 C. R. Shaddix, 8367

1	MS 9052	L. G. Blevins, 8367
3	MS 9018	Central Technical Files, 8945-1
1	MS 0899	Technical Library, 9616
1	MS 9021	Classification Office, 8511 for Technical Library, MS 0899, 9616 DOE / OSTI via URL